4

GL-TR-90-0086

AD-A224 266

Rg Waves as a Depth Discriminant for Earthquakes and Explosions in New England

Alan L. Kafka

Weston Observatory
Dept. of Geology and Geophysics
Boston College
Weston, MA 02193

April 10, 1990

Final Report
24 October 1989-31 December 1989

Approved for public release; distribution unlimited

Geophysics Laboratory
Air Force Systems Command
United States Air Force
Hanscom AIr Force Base, Massachusetts 01731-5000

SPONSORED BY
Defense Advanced Research Projects Agency
Nuclear Monitoring Research Office
ARPA ORDER NO 5299

MONITORED BY
Geophysics Laboratory
F19628-87-K-0004

The views and conclusions contained in this document are those of the authors and should not be interpreted as representing the official policies, either expressed or implied, of the Defense Advanced Research Projects Agency or the U.S. Government.

This technical report has been reviewed and is approved for publication.

JAMES F. LEWKOWICZ
Contract Manager
Solid Earth Geophysics Branch
Earth Sciences Division

JAMES F. LEWKOWICZ
Branch Chief
Solid Farth Geophysics Branch
Earth Sciences Division

FOR THE COMMANDER

DONALD H. ECKHARDT, Director
Earth Sciences Division

This report has been reviewed by the ESD Public Affairs Office (PA) and is releasable to the National Technical Information Service (NTIS).

Qualified requestors may obtain additional copies from the Defense Technical Information Center. All others should apply to the National Technical Information Service.

If your address has changed, or if you wish to be removed from the mailing list, or if the addressee is no longer employed by your organization, please notify GL/IMA, Hanscom AFB, MA 01731-5000. This will assist us in maintaining a current mailing list.

Do not return copies of this report unless contractual obligations or notices on a specific document requires that it be returned.

REPORT DOCUMENTATION PAGE

Form Approved
OMB No. 0704-0188

1. AGENCY USE ONLY *(Leave blank)*

2. REPORT DATE
10 April 1990

3. REPORT TYPE AND DATES COVERED
Scientific
Final 24 Oct 1989 - 31 Dec 1989

4. TITLE AND SUBTITLE
Rg Waves as a Depth Discriminant for Earthquakes and Explosions in New England

5. FUNDING NUMBERS
C: F19628-87-K-0004
PE: 61101E
PR: 7A10
TA: DA
WU: CT

6. AUTHOR(S)
Dr. Alan L. Kafka

7. PERFORMING ORGANIZATION NAME(S) AND ADDRESS(ES)
Weston Observatory
Boston College
381 Concord Road
Weston, MA 02193

8. PERFORMING ORGANIZATION REPORT NUMBER

9. SPONSORING/MONITORING AGENCY NAME(S) AND ADDRESS(ES)
Geophysics Laboratory
Hanscom AFB, MA 01731-5000

Contract Manager: James Lewkowicz/LWH

10. SPONSORING/MONITORING AGENCY REPORT NUMBER
GL-TR-90-0086

11. SUPPLEMENTARY NOTES

12a. DISTRIBUTION/AVAILABILITY STATEMENT
Approved for Public Release
Distribution Unlimited

12b. DISTRIBUTION CODE

13. ABSTRACT
Fundamental mode Rayleigh waves with periods between about 0.4 and 2.5 sec (Rg) are often observed on seismograms of explosions and very shallow-focus earthquakes. In this study, Rg waves generated by small earthquakes and explosions in New England were investigated to evaluate the extent to which Rg waves can be used to estimate depth. The strongest Rg signals recorded in New England are generally in the period range of 0.5 to 1.5 sec. In that period range, Rg displacement is essentially confined to the upper 5 km of the crust, with most of the Rg wave energy in the upper 2 or 3 km. Sources deeper than about 4 km would not be expected to generate strong Rg signals at these periods; and so, if Rg can be clearly identified on a seismogram, the source is most likely very shallow. Observed Rg waves can, therefore, be used to discriminate very shallow-focus events from deeper events, provided that Rg can be identified and distinguished from other phases. A method for identifying Rg waves at distances up to about 170 km is presented in this report. Rg is identified and distinguished from other phases by measuring amplitudes at particular periods and arrival times using a narrow bandpass filter analysis. Rg/P and Rg/Lg ratios are estimated by forming the ratios of amplitudes in the appropriate group velocity frequency windows. An Rg/Lg ratio appears to be a better measure of the presence of Rg on a seismogram than an Rg/P ratio. Observed Rg/Lg ratios are used to estimate depths of two earthquakes recorded by the NESN. (EDC)

14. SUBJECT TERMS
Rg waves as a depth discriminant
Characteristics of Rg wave recorded in New England

15. NUMBER OF PAGES
56

16. PRICE CODE

17. SECURITY CLASSIFICATION OF REPORT	18. SECURITY CLASSIFICATION OF THIS PAGE	19. SECURITY CLASSIFICATION OF ABSTRACT	20. LIMITATION OF ABSTRACT
UNCLASSIFIED	UNCLASSIFIED	UNCLASSIFIED	UNCLASSIFIED

TABLE OF CONTENTS

TECHNICAL SUMMARY

Fundamental mode Rayleigh waves with periods ranging from about 0.2 to 2.5 sec (Rg) are often observed on seismograms of explosions and very shallow-focus earthquakes in New England as well as in other parts of the world. The Rg phase is particularly prominent on vertical component seismograms of quarry blasts. In this study, I investigated Rg waves generated by small earthquakes and explosions recorded at stations of the New England Seismic Network (NESN) operated by Weston Observatory. The strongest Rg signals recorded by the NESN are generally in the period range of about 0.5 to 1.5 sec. In that period range Rg displacement is essentially confined to depths of about 1 to 5 km, with most of the Rayleigh wave energy in the upper 2 or 3 km. Thus, sources deeper than about 4 km would not be expected to generate strong Rg signals; and so, if Rg can be clearly identified on a seismogram, the source is most likely very shallow. Observed Rg waves can, therefore, be used to discriminate very shallow-focus events from deeper events, provided that the Rg phase can be identified and distinguished from other recorded phases.

The objectives of this study were: (1) to study the characteristics of Rg waves recorded in New England and therefore determine how to identify Rg on a seismogram and how to distinguish it from other recorded phases; and (2) to compare amplitudes of Rg waves recorded from events at various depths with amplitudes of other recorded phases, such as P and Lg. A major part this study involved developing a method for identifying Rg waves and distinguishing them from other recorded phases. That method involves measuring amplitudes of seismic wave energy at particular periods and arrival times using a narrow bandpass filter analysis. The appropriate periods and arrival times are chosen for different phases, and amplitude ratios are formed to estimate the relative amount of energy recorded for different phases.

The results of testing this narrow bandpass filter method on a sample of earthquakes, quarry blasts and refraction blasts in New England indicate that at NESN stations, Rg appears to be limited primarily to the frequency band of 0.7 to 2.0 Hz, and Rg arrives with group velocities between about 2.2 and 3.3 km/sec. It is generally difficult to distinguish Sg waves from Lg waves on NESN seismograms because at the high frequencies that are recorded (about 3.0 to 12.0 Hz), the Sg and Lg waves arrive as a rather complicated wave train with group velocities between about 3.0 and 3.7 km/sec. The term "Lg", used in this report, refers to this complicated "Sg and Lg" wave train. An Rg/P ratio and an Rg/Lg ratio are estimated by forming the ratios of amplitudes of energy in the appropriate group velocity - frequency windows. The Rg/Lg ratio appears to be a better measure of the presence of Rg on a seismogram than the Rg/P ratio. Most of the Rg seismograms analyzed in this study have been from distances of less than 130 km from the source. This distance limitation is due primarily to the small size of most quarry blasts recorded in New England (m_{bLg} ~1.0 to 1.5) and to the relatively low dynamic range and narrow-band response of the NESN instruments. Quite often, none of the regional phases are very well recorded at distances beyond about 150 km from these small events. For the largest quarry blasts, however, Rg has been recorded at distances up to about 170 km, and if an event is clearly recorded at that distance, the Rg/Lg ratio method appears to work as well as it does at shorter distances. Higher-quality stations with broader-band response and greater dynamic range should be able to detect Rg waves at even greater distances, especially from more energetic sources.

Rg AS A DEPTH DISCRIMINANT FOR EARTHQUAKES AND EXPLOSIONS:

A CASE STUDY IN NEW ENGLAND

Alan L. Kafka
Weston Observatory
Department of Geology and Geophysics
Boston College
Weston, MA 02193

Bulletin of the Seismological Society of America (1990)

Vol. 80, No. 2, 373-394

ABSTRACT

Fundamental mode Rayleigh waves with periods between about 0.4 and 2.5 sec (Rg) are often observed on seismograms of explosions and very shallow-focus earthquakes. The Rg phase is particularly prominent on seismograms of quarry blasts. In this study, Rg waves generated by small earthquakes and explosions in New England are investigated to evaluate the extent to which Rg waves can be used to estimate depths of events in the upper crust. The data were recorded by the New England Seismic Network (NESN) operated by Weston Observatory. The strongest Rg signals recorded by the NESN are generally in the period range of 0.5 to 1.5 sec. In that period range, Rg displacement is essentially confined to the upper 5 km of the crust, with most of the Rg wave energy in the upper 2 or 3 km. Sources deeper than about 4 km would not be expected to generate strong Rg signals at these periods; and so, if Rg can be clearly identified on a seismogram, the source is most likely very shallow. Observed Rg waves can, therefore, be used to discriminate very shallow-focus events from deeper events, provided that Rg can be identified and distinguished from other phases.

A method for identifying Rg waves at distances up to about 170 km is presented in this paper. Rg is identified and distinguished from other phases by measuring amplitudes at particular periods and arrival times using a narrow bandpass filter analysis. Rg/P and Rg/Lg ratios are estimated by forming the ratios of amplitudes in the appropriate group velocity - frequency windows on vertical component seismograms. The phase referred to as "Lg" is actually a complicated wave train recorded on short-period seismograms that travels with group velocities appropriate for S and Lg waves. An Rg/Lg ratio appears to be a better measure of the presence of Rg on a seismogram than an Rg/P ratio. Observed Rg/Lg ratios are used to estimate depths of two earthquakes recorded by the NESN.

INTRODUCTION

Fundamental mode Rayleigh waves with periods ranging from about 0.4 to 2.5 sec (Rg) are often observed on seismograms of explosions and very shallow-focus earthquakes in New England as well as in other parts of the world. Since Rg is a fundamental mode surface wave, it is not surprising that near-surface and very shallow-focus sources generate strong Rg signals. Based on the principles of surface wave and body wave excitation, Båth (1975) proposed that Rg could be used as a depth discriminant for events recorded at local and regional distances. The principles underlying the use of Rg as a depth discriminant are that Rg amplitudes are very dependent on source depth, while amplitudes of other recorded phases such as Pg and Sg are, on average, less dependent on depth. Although these principles are straight forward, applying them to actual data can be problematic because of the complexity of short-period local and regional seismograms.

In this paper, I investigate seismograms of earthquakes and explosions recorded in New England to evaluate the extent to which Rg waves can be used as a depth discriminant for regionally recorded events. Specifically, observed amplitudes of Rg waves recorded by the New England Seismic Network (NESN; Figure 1) are compared with the amplitudes of other recorded phases to test how effectively such comparisons work as a depth discriminant.

The strongest Rg signals recorded by the NESN are generally in the period range of about 0.5 to 1.5 sec (Figure 2). In that period range, Rg displacement is essentially confined to depths of about 1 to 5 km, with most of the Rayleigh wave energy in the upper 2 or 3 km (Figure 3). Thus, sources deeper than about 4 km would not be expected to generate strong Rg signals; and, if Rg can be clearly identified on a seismogram, the source is most likely very shallow. The task of developing a method for using Rg as a depth discriminant is therefore (to a large extent) a matter of developing a method for identifying the Rg phase and distinguishing it from other phases.

As with other regional discriminants, there are a number of reasons why using Rg as a depth discriminant is not as simple as the underlying principles suggest. For example, Rg waves are likely to experience significant attenuation resulting from low Q material in the shallow crust. In addition, the radiation patterns of Rg are likely to be asymmetric for earthquakes (and possibly also asymmetric for some quarry blasts). Thus, the lack of observed Rg waves is not necessarily indicative of a deep source. In spite of such problems, this paper illustrates that, at least in areas of New England where this study was conducted, Rg waves do have practical value as a depth discriminant. In practical situations, Rg might be used as one of several regional discriminants, none of which are likely to be without their own shortcomings.

Most of the sources in this study were quarry blasts and small earthquakes recorded in southern New England. A few additional sources were refraction blasts detonated in Maine during 1984 by the U.S Geological Survey. Locations and origin times of the sources analyzed in this study are listed in Tables 1 and 2.

CHARACTERISTICS OF Rg WAVES RECORDED IN NEW ENGLAND

Although local and regional phases recorded by the NESN are generally quite complicated, the Rg phase is often a relatively simple, dispersed wave train. This dispersion appears to be caused by low seismic velocities in the upper few km of the crust--presumably due to weathering of shallow crustal rocks (e.g. Båth, 1975; Kafka and Dollin, 1985; Kafka and Reiter, 1987).

Figure 2 shows seismograms and amplitude spectra from three quarry blasts and one earthquake recorded in New England at distances ranging from 36 to 74 km. The Rg phase is prominent on the seismograms of the quarry blasts, but it is absent on the seismogram of the earthquake. The earthquake had a fairly well-constrained depth of about 5 km (see below), and the lack of an Rg wave is consistent with the idea that the earthquake was too deep to generate significant Rg wave energy.

The prominent spectral peaks located between about 1.5 and 0.5 sec (0.67 and 2.00 Hz) in Figures 2(a)-2(c) are characteristic of NESN seismograms of quarry blasts. These spectral peaks were interpreted by Filipkowski (1986) and Kafka (1987) as characteristic of Rg waves. If a low-frequency spectral peak is indeed characteristic of Rg, one way to identify Rg on a seismogram would be to calculate an amplitude ratio that compares amplitudes in that low-frequency band with amplitudes in other frequency bands. Such an amplitude ratio discriminant is simple and straight forward to apply, but it ignores some of the expected characteristics of the seismograms. In particular, differences in arrival times of various regional phases and the dispersion of Rg should be considered as part of the identifying characteristics of regional phases.

In this paper, I suggest a method of identifying the Rg phase that takes into account the arrival times of Rg and other regional phases. The method involves comparing amplitudes in the part of the seismogram where the Rg wave energy is expected to arrive with amplitudes in the part of the seismogram where P, S and Lg wave energy is expected to arrive. The amplitudes in the various arrival time windows are measured for specific periods using a narrow bandpass filter (NBF) analysis (Dziewonski et al., 1969).

For many of the seismograms analyzed in this paper, the paths were from areas where the shallow crust has a relatively simple structure and where there is relatively minor lateral variation in shallow crustal structure. Indeed, one of the reasons for choosing the parts of New England used for this study was that they consist of relatively simple shallow crustal structures (and relatively low topography). More complex structure and extensive topographic relief should cause scattering of Rg and might convert Rg into body waves and other types of surface waves (e.g. McLaughlin and Jih, 1987). The Rg waveforms in such a region would be more complex, and the amount of Rg energy (relative to other phases) at a given distance from the source would be less. It is therefore important to recognize that, strictly speaking, the results of this study can only be applied to regions where characteristics of Rg wave propagation are well-known.

EXCITATION OF Rg WAVES FOR SOURCES BURIED AT VARIOUS DEPTHS IN THE UPPER CRUST

The idea of using Rg as a depth discriminant is based on the principle that, for periods near 1 sec, the energy of fundamental mode Rayleigh waves is concentrated in the upper few kilometers of the crust. Figure 3 shows displacement versus depth for the vertical component Rg wave calculated for a model of the upper crust in New England. Similar calculations were performed using numerous (flat-layered) models, and the results suggest that displacement versus depth of Rg is not very dependent on differences in upper crustal structure. Thus I assume, for the purpose of this study, that a reasonable estimate of the crustal structure in a given area is sufficient for estimating the level of excitation of Rg for sources buried at varying depths.

To test the idea of using Rg as a depth discriminant on actual data, it is important to identify events with well-constrained depths recorded at a range of distances and azimuths. Identifying such events was one of the difficult parts of this study. The relatively sparse distribution of stations and the low level of earthquake activity make it difficult to find earthquakes in the study area that are recorded by several nearby stations. Two earthquake sequences for which good depth estimates were available from aftershock surveys are the 1987 Moodus, CT earthquakes and the 1985 Ardsley, NY earthquakes. In this study, the Moodus earthquakes are assumed to be 1.6 km deep, and the Ardsley earthquakes are assumed to be 5.2 km deep (see Table 2). Other events in this study are quarry and refraction blasts (which are known to occur at the surface) and several earthquakes whose depths are poorly constrained. Although these earthquakes may have occurred almost anywhere in the upper half of the crust (e.g. Ebel and Kafka, 1989), they are obviously buried at some depth below the surface.

USING NARROW BANDPASS FILTER ANALYSIS TO IDENTIFY Rg

This section presents a method of identifying Rg and comparing Rg amplitudes to amplitudes of P, S and Lg waves recorded on the same seismogram. In this method, amplitudes are measured at particular periods and arrival times using an NBF analysis. Figure 4(a) shows an NBF analysis of a seismogram with a very prominent Rg wave as well as prominent arrivals in the S and Lg arrival time windows. Since S and Lg waves are difficult to separate at these distances and frequencies, the notation "Lg" will (in the remainder of this paper) refer to the entire wave train from the onset of the S wave to the end of the S and Lg coda, and S and Lg are analyzed as one (complicated) wave train.

The seismogram shown in Figure 4(a) has high amplitudes in both the Lg and Rg arrival time - frequency windows. The situation is different for the seismogram in Figure 4(b) where Rg has much larger amplitudes than Lg. In the example shown in Figure 4(c), the event is too deep to generate significant Rg energy, so the shaded area is limited to where Lg is expected to arrive.

The seismogram of the Erving, MA earthquake (Table 2) recorded at station WES has a small (but observable) Rg wave. An NBF analysis of that seismogram is shown in Figure 5(a). Relatively high amplitudes are observed in both the Lg and the Rg parts of the velocity-period plane of the Erving, MA - WES seismogram.

These examples suggest that the ratios of Rg amplitudes to Lg or P wave amplitudes can be estimated by narrow bandpass filtering each seismogram and then taking the ratios of amplitudes within the appropriate velocity-period windows. To do this, it is necessary to estimate the group velocity dispersion of Rg waves in the area being investigated.

Rg Dispersion in New England. One of the reasons for choosing New England for this case study is that group velocity dispersion of Rg waves is fairly well-known in that region (e.g. Kafka and Dollin, 1985; Kafka and Reiter, 1987; Kafka, 1988). Figure 5(b) shows a summary of results of Rg dispersion studies in southern New England (SNE), where most of the Rg investigations conducted at Weston Observatory have taken place. Results for northern New England are not as complete as those shown in Figure 5(b), but Rg dispersion results are available from a study of southeastern Maine (Kafka and Reiter, 1987). In that study, we found evidence for lateral anisotropy in the shallow crust, and although the relationship between geology and Rg dispersion is quite different in Maine than in SNE, the total range of Rg group velocities is approximately the same in both regions.

There appear to be systematic regional differences in Rg dispersion in New England (see Kafka and Reiter, 1987 and Kafka, 1988 for more detailed discussions of this topic). Taking such regional variations into account should ultimately help in identifying the Rg phase, but for the purpose of this paper such an approach would yield a very small number of observations for a given sub-region. While it would have been easier to identify the appropriate arrival time window for Rg waves if the study was limited to paths within a specific sub-region, such an approach would have severely limited the number of seismograms available for this analysis. Although I did exclude paths across the Hartford dispersion region where group velocities are very low (presumably due to glacial sediments overlying Mesozoic sedimentary rocks), I considered the full range of observed group velocities for all crystalline basement paths when attempting to identify the expected arrival times of Rg waves. This made it possible to classify all of the seismograms from this study into only two subsets, one subset for earthquakes and another for blasts (Tables 3 and 4).

Calculating Rg/Lg and Rg/P Ratios. This section describes how I estimate the ratio of Rg amplitudes to amplitudes of Lg and P waves using an NBF analysis. The amplitudes are entered into a matrix [Figure 5(c)], with a given cell representing the amplitude at a particular point on the velocity-period plane. All amplitudes in the cells labelled P are averaged to give an estimate of the average P wave amplitude. Similarly, the amplitudes in the cells labelled Lg and Rg are averaged to give an estimate of the average Lg and Rg amplitudes, respectively. In addition, the cells corresponding to a given wave type are searched to find the maximum amplitude for each wave type. The following four ratios are then calculated (see Tables 3 and 4):

(1) Rg/Lg (AV) = Rg(average)/Lg(average)
(2) Rg/P (AV) = Rg(average)/P(average)
(3) Rg/Lg (MAX) = Rg(maximum)/Lg(maximum)
(4) Rg/P (MAX) = Rg(maximum)/P(maximum)

The specific choice of which cells to use for each wave type is, of course, empirical. Expected arrival times and periods for Rg waves are based on the range of observed group velocities discussed above. Expected arrival times and periods for Lg and P waves are based on the range of first arrival velocities and the frequency content for each of those phases that is typically observed in New England.

Figure 6 shows histograms of the logarithm of all four ratios calculated from seismograms of blasts (zero depth) and from seismograms of the Ardsley, NY earthquakes (5.2 km depth). The only ratio for which there is no overlap between the populations for the blasts and the earthquakes is Rg/Lg (AV). Thus, the Rg/Lg (AV) ratio appears to be the best of the four ratios to use as a measure of the presence of Rg on a seismogram.

The observation that an Rg/Lg ratio appears to be a better measure of the presence of Rg on a seismogram than an Rg/P ratio is consistent with the results of Langston (1987). He calculated synthetic seismograms for sources at various depths in a layered half-space model of the upper crust, and measured Rg, S and P amplitudes from the synthetic seismograms. Langston found that the Rg/S ratio was a more robust measure of source depth than the Rg/P ratio.

Based on this analysis of the blasts and the Ardsley, NY earthquakes, I decided to use Rg/Lg (AV) as a measure of the presence of Rg wave energy on a seismogram. In the discussion that follows, the notation "Rg/Lg" is used to refer to Rg/Lg (AV).

Figures 7 shows histograms of the logarithm of the Rg/Lg ratios for blasts and for the Moodus, CT; Erving, MA; and the Boxboro, MA earthquakes, respectively. All of the ratios for the Moodus, CT earthquake overlap with those of the blasts. That is not surprising, since that earthquake is known to be very shallow. The average value of Rg/Lg for the Moodus earthquake (0.93) is lower than the average value for the blasts (2.50), which is consistent with the 1.6 km depth of the earthquake.

The Erving, MA earthquake ratios do not overlap with those of the blasts, and the average value of Rg/Lg was 0.22 for that earthquake. These ratios for the Erving, MA event are almost as low as those of the Ardsley, NY earthquakes (average Rg/Lg = 0.16), which may indicate that the Erving, MA earthquake was more than a few km deep. However, the presence of a low amplitude Rg wave on the seismogram recorded at WES (Figure 5) implies that the depth of that earthquake was probably less than about 4 km.

The Boxboro, MA earthquake ratios cluster around the lower end of the ratios for the blasts, and the average value of Rg/Lg for that earthquake was 0.86. These somewhat higher values for the Rg/Lg ratio (similar to the values found for the Moodus earthquake) suggest that the Boxboro earthquake was a shallow event. Also, several of the seismograms of the Boxboro earthquake exhibited clearly recorded Rg waves (Figure 8), further indicating that this event was shallow (perhaps no deeper than about 2 km).

DISTANCE LIMITATION FOR Rg METHODS AND TEST OF STATISTICAL SIGNIFICANCE

Most of the seismograms discussed in this paper were recorded at distances of less than 100 km, and a few were recorded as close as 17 km from the sources. If Rg is to be of practical value as a depth discriminant, it is important to ask how close a station must be to the source in order to use Rg as a depth discriminant. One point to be noted in this regard is that the quarry blasts discussed in this paper are quite small (m_{bLg} ~1.0 to 1.6), so that none of the seismic phases are recorded very far from the source. Figure 8(a) shows seismograms of two of the larger quarry blasts from this study. For those blasts, Rg and other phases were recorded at distances of 155 and 168 km. For both of the seismograms in Figure 8(a), the Rg/Lg ratio (1.34 and 1.96) is lower than the average value of all the Rg/Lg ratios for blasts (2.50), but is about the same as the average of the Rg/Lg ratios determined from stations that were at least 50 km from the blasts (1.58).

Once a blast is known to have occurred at a particular quarry, its location is known accurately. Earthquakes, on the other hand, must be large enough to be recorded at many stations in order to be located accurately enough to be used in this study. Thus, the earthquakes in this study were generally larger than the quarry blasts, and the epicentral distances for the earthquakes were, on average, larger than for the blasts. Figure 9 shows the distribution of epicentral distances for the earthquake and blast seismograms. In an effort to analyze seismograms at a similar range of distances, I attempted to find as many seismograms of blasts as possible that were recorded at greater distances.

Also shown in Figure 9 is the Rg/Lg ratio for the blasts as a function of distance from the source, along with a best fitting least squares line. Certainly there is a trend downward, which is probably due to a greater loss of Rg wave energy than Lg wave energy at the greater distances. However, it appears that this distance effect has not obscured the identification of Rg to a very large extent, since all of the seismograms of the Ardsley, NY earthquakes (5.2 km depth) had values of Rg/Lg that were lower than the values found for the blasts [Figure 6(a)]. The two samples shown in Figure 6(a) included stations as far away as 129 km for the earthquakes and 168 km for the blasts.

The effect of distance on the Rg/Lg ratios appears to be much less significant in the distance range of 50 to 170 km [Figure 9(d)]. Thus it seems appropriate to compare Rg/Lg ratios determined from seismograms of blasts recorded in the 50-170 km distance range to the data set of Rg/Lg ratios for earthquakes (all of which were recorded within the 50-170 km range). Although this procedure lowers the number of ratios that can be analyzed for blasts to only 24 samples, it is desirable to compare blast and earthquake ratios from a distance range within which Rg/Lg does not appear to be very dependent on distance.

A statistical analysis was used to test the difference between the Rg/Lg ratios for the entire data set of earthquakes and the Rg/Lg ratios for the data set of blasts recorded in the 50-170 km distance range. Since all of the earthquakes occurred at some depth below the surface and all of the blasts occurred at zero depth, one would expect that, if the Rg/Lg ratio is a measure of the presence of Rg waves, the earthquake ratios should generally be lower than the blast ratios. I used a non-parametric test (the Mann-Whitney U-test) that does not require the assumption that the distributions of ratios are normally distributed (Hinkle et al., 1979). The null hypothesis was that the median of the earthquake ratios was the same as the median of the blast ratios, and the alternative hypothesis was that the median of the earthquake ratios was lower. Applying the Mann-Whitney test to evaluate the statistical significance of the difference between the medians of the earthquake and blast ratios, I found that the median of the Rg/Lg ratios for earthquakes is lower than that for blasts at the 99% confidence level.

ESTIMATING DEPTH FROM Rg/Lg RATIOS

The ultimate goal of this study is to develop a method for estimating depths of regionally recorded sources from observed amplitudes of Rg and other phases. This section presents a method for estimating depth that is based on the Rg/Lg ratios discussed above. The approach taken here is similar to that of Båth (1975), although his observed ratios were based on trace amplitudes rather than spectral amplitudes.

Let r(h) represent the average Rg/Lg ratio for an earthquake at depth h, and let r(0) represent the average ratio for sources located at the surface. The specific value of r(h) for a given earthquake will depend on a number of factors (in addition to depth) including: the level of excitation of the different wave types that are generically referred to as "Lg", the attenuation (and geometrical spreading) of the different wave types that contribute to the Rg/Lg ratio, the range of azimuths and distances at which recordings are available, the focal mechanism, and the instrument response. For the purpose of this case study, I am assuming that (in the 50-170 km distance range) all of the factors contributing to the average Lg wave amplitude are, on average, not very dependent on depth (provided that data are available at a range of azimuths). However, the Rg amplitude varies by more than order of magnitude between events located at the surface and events at about 5 km depth (Figure 3). Furthermore, I assume that the variation in Rg amplitude with depth is approximately characterized by the 0.8 sec displacement-depth eigenfunction. Since the eigenfunction is normalized to be 1.0 at the surface, the observed ratios are normalized by dividing them by r(0) (1.58 in this case), and the resulting values (Table 5) are referred to $r_n(h)$. If f(h) is the eigenfunction, then an approximation to $r_n(h)$ will be:

$$r_n(h) = f(h) + K \qquad (1)$$

where K is the value of $r_n(h)$ for an event deeper than 5.0 km. K is likely to be greater than zero because there is probably some energy in the various arrival time -

frequency windows even when no Rg wave is present. For this illustration, I use 0.10 (the average Rg/Lg ratio for the Ardsley, NY earthquakes) as an estimate of K.

The depth of an earthquake can therefore be estimated by finding the value of h that satisfies equation (1). For the earthquakes in this case study, the depths estimated from the Rg/Lg ratios using equation (1) are given in Table 5.

DISCUSSION AND CONCLUSIONS

As is clear from the examples described above, there are some practical problems associated with using Rg as a depth discriminant. Nonetheless, regional seismograms are generally complex, and it is unlikely that <u>any</u> regional discriminant will work in all cases. It does, however, seem clear that, at least in the parts of New England where this study was conducted, Rg waves have some practical value as a depth discriminant.

The ratio determined by dividing the average amplitude in the Rg wave arrival time - frequency window by the average amplitude in the Lg wave arrival time - frequency window was the best measure that I was able to find for determining whether Rg is present on a seismogram. For the Ardsley, NY earthquakes, all of the seismograms yielded an Rg/Lg ratio that was lower than any Rg/Lg ratio found for blasts, which is consistent with the 5.2 km depth of those earthquakes. The Moodus, CT earthquake yielded Rg/Lg ratios that overlapped with the ratios determined for the blasts, which is consistent with the 1.6 km depth of that earthquake. Thus, at least in these two cases, the observed seismograms are generally consistent with what might be expected from the theory of surface wave and body wave excitation. In addition, using all seismograms recorded in the 50-170 km distance range, the difference in Rg/Lg ratios for blasts and earthquakes was found to be statistically significant at the 99% confidence level.

Based on equation (1), the Boxboro, MA and Erving, MA earthquakes were found to have depths of 1.2 and 3.0 km, respectively. These depths were determined from five stations at distances of 75 to 136 km for the Boxboro earthquake and from five stations at distances of 85 to 131 km for the Erving earthquake. With that type of station distribution, it would not be possible to constrain such shallow depths based on arrival times of P and S waves. For such cases, some type of body waveform discriminant, such as the sP method described by Langston (1987) would also be helpful.

In regions where there is more complex structure in the shallow crust and where there is a great deal of topographic relief, Rg might not be as good a discriminant as it would be in New England. Just how complex an area would have to be to totally rule out the use of Rg as a depth discriminant can only be determined by performing similar analyses in other regions. However, in any region where event depth must be determined from a limited number of seismic observations, it seems that some measure of the presence (or absence) of Rg wave energy on seismograms should be considered as a possible depth discriminant for events in the upper crust.

ACKNOWLEDGMENTS

This research was initiated when the author was a National Research Council Associate at the Air Force Geophysics Laboratory, Hanscom AFB, MA. Most of the support for this study was provided by the Defense Advanced Research Projects Agency under contract #F19628-87-K-004. Additional support was also provided by the Air Force Office of Scientific Research under Grant AFOSR 85-0177 and the National Science Foundation under Grant EAR-8606404.

REFERENCES

Bath, M. (1975). Short-period Rayleigh waves from near-surface events, Phys. Earth Planet. Int., 10, 369-376.

Chiburis, E.F., R.O. Ahner, and T. Graham (1977). Preliminary travel time model of southern New England (abstract), Earthquake Notes, 48, 11.

Dziewonski, A.M., S. Bloch and M. Landisman (1969). A technique for the analysis of transient seismic signals, Bull. Seis. Soc. Am., 59, 427-444.

Ebel, J.E. and A.L. Kafka (1988). Earthquake activity in the northeastern United States, in Slemmons, D.B., Engdahl, E.R., Blackwell, D., and Schwartz, D., Neotectonics of North America, in press, The Geological Society of America, CSMV-1, Boulder, Colorado.

Filipkowski, F. J. (1986). The Use of Short-Period Rg Waves as a Depth Discriminant for Seismic Events in the Upper Crust of the Northeastern United States, Master's Thesis, Boston College, Chestnut Hill, Massachusetts, 81 pp.

Hinkle, D.E., W. Weirsma, and S.G. Jurs (1979). Applied Statistics for Behavioral Sciences, Houghton Mifflin Company, Boston, Massachusetts.

Kafka, A.L. (1988). Earthquakes, geology and crustal features in southern New England, Seism. Res. Let., 59(4), 173-181.

Kafka, A.L. (1987). Rg waves as a depth discriminant for earthquakes and explosions in New England, 9th Annual Defense Advanced Research Projects Agency/ Air Force Geophysics Laboratory Symposium, Nantucket, MA, June 1987, 236-241.

Kafka, A. L. and M. F. Dollin (1985). Constraints on Lateral Variation in Upper Crustal Structure beneath Southern New England from the Dispersion of Rg Waves, Geophys. Res. Lett., 12, 235-238.

Kafka, A.L. and E.C. Reiter (1987). Dispersion of Rg waves in southeastern Maine: evidence for lateral anisotropy in the shallow crust, Bull. Seis. Soc. Am., 77, 925-941.

Kafka, A.L. and E.C. Reiter (1988). Seismic velocity structure of the shallow crust in southern New England from dispersion of Rg waves (abstract), EOS, Trans. Am. Geophys. Un., 69(16), 495.

Langston, C.A. (1987). Depth of faulting during the 1968 Meckering, Australia earthquake sequence determined from waveform analysis of local seismograms, J. Geophys. Res., 92, 11,561-11,574.

Locke, K. (1985). Quarterly Seismicity Bulletin of the New York - New Jersey Network, 1 October - 31 December 1985, Published by Lamont-Doherty Geological Observatory of Columbia University, Palisades, NY.

McLaughlin, K.L. and R.-S. Jih (1987). Finite-difference simulations of Rayleigh-wave scattering by shallow heterogeneity, Report AFGL-TR-87-0322, TGAL-87-02, Teledyne Geotech, Alexandria, VA.

Mrotek, K.A., R.C. Quittmeyer, P.G. Naumoff and C.T. Statton (1988). Observations of the earthquake swarm near Moodus, Connecticut: September/October 1987 (abstract), EOS, Trans. Am. Geophys. Un., 69(16), 495.

Saito, M. (1967). Excitation of free oscillations and surface waves by a point source in a vertically heterogeneous earth, J. Geophys. Res., 72, 3689-3699.

TABLE 1

QUARRY AND REFRACTION BLASTS
($1.0 < m_{bLg} < 1.6$)

Code	Location	Date	Origin Time	RMS	Lat	Long
LT1	Littleton, MA	07/15/87	196:18:59:55.345	*	42.555	71.521
LT13	Littleton, MA	06/11/85	162:18:47:20.1	.22	42.555	71.521
LT17	Littleton, MA	10/24/85	297:16:22:58.0	.25	42.555	71.521
NB2	North Branford, CT	07/01/85	182:14:29:59.6	.25	41.333	72.767
NB6	North Branford, CT	08/27/85	239:14:45:00.8	.39	41.333	72.767
RG1	Reed Gap, CT	08/31/85	243:14:30:04.2	.25	41.471	72.735
RG4	Reed Gap, CT	08/06/85	219:14:20:00.4	.29	41.471	72.735
RG5	Reed Gap, CT	07/17/85	198:14:49:58.0	.23	41.471	72.735
MB04	Maine - SP#4	10/18/84	292:06:02:00.007	*	44.763	69.796
MB06	Maine - SP#6	09/25/84	269:05:33:00.006	*	44.462	69.232
MB07	Maine - SP#7	10/04/84	278:04:03:00.009	*	44.327	68.980
MB15	Maine - SP#15	10/18/84	292:04:20:00.007	*	44.977	69.593
MB16	Maine - SP#16	10/18/84	292:06:00:00.007	*	45.107	69.382

* timed blasts
SP = Shot Point

TABLE 2

EARTHQUAKES

Location (Code)	Date	Origin Time	RMS	Lat, Long	Depth	m_C*	m_N*	m_{bLg}
Ardsley, NY (ARDF, foreshock)	10/19/85	292:10:05:45.35	0.33	40.994, 73.787	5.2†	2.4		
Ardsley, NY (ARDA, aftershock)	10/21/85	294:10:37:14.91	0.14	40.981, 73.842	5.2†	3.0		2.9
Boxboro, MA (BXBR)	10/15/85	288:20:00:38.64	0.40	42.540, 71.458	?	2.9	3.1	
Erving, MA (ERVG)	06/14/84	166:20:56:33.93	0.54	42.590, 72.400	?	2.4	2.7	2.1
Moodus, CT (MDUS)	09/11/87	254:14:46:33.97	0.20	41.529, 72.447	1.6††	2.9	2.4	

* m_N and m_C are local magnitudes that are used for reporting magnitudes of earthquakes recorded by seismic networks in the northeastern U.S. m_N is calculated from amplitudes of high-frequency Lg waves, and m_C is calculated from signal duration. m_N and m_C tend to overestimate m_{bLg} by a few tenths of a magnitude unit (Kafka, 1988).

† Average depth from aftershock survey reported by Locke (1985).

†† Midrange of depths from aftershock survey of Mrotek et al. (1988).

TABLE 3

Rg/Lg AND Rg/P RATIOS FOR BLASTS

Event-Station	Distance (km)	Rg/Lg(AV)	Rg/P(AV)	Rg/Lg(MAX)	Rg/P(MAX)
LT1-MD1	136.0	1.73	3.05	2.30	3.59
LT1-MD2	136.8	0.41	0.47	0.48	0.52
LT1-MD3	140.5	1.23	1.61	0.98	1.43
LT1-MD4	142.8	1.06	1.51	1.75	1.45
LT1-NSC	122.4	1.88	2.52	2.29	3.04
LT1-QUA	71.0	1.04	1.87	2.14	2.52
LT1-WES	25.0	3.69	4.84	7.23	10.00
LT13-NSC	122.4	3.24	4.15	3.40	4.72
LT13-QUA	71.0	1.31	2.55	2.24	3.61
LT13-WES	25.0	10.67	9.40	11.56	8.73
LT17-MD3	140.5	1.90	2.33	3.02	3.21
LT17-QUA	71.0	3.91	3.87	4.99	5.22
LT17-WES	25.0	13.52	13.46	13.30	18.32
MB04-HKM	17.3	1.64	2.18	1.26	1.56
MB06-HKM	39.0	2.51	1.48	6.67	1.33
MB07-HKM	63.9	0.56	0.95	1.02	1.45
MB15-MIM	52.6	1.12	3.19	1.46	5.74
MB16-MIM	31.0	0.56	1.57	1.05	2.49
NB1-BCT	62.6	1.32	1.02	1.52	0.79
NB2-HDM	27.1	2.87	6.88	2.02	6.37
NB2-MD1	35.5	4.25	14.65	3.13	6.61
NB2-WES	168.0	1.34		2.94	
NB3-BCT	62.6	1.67	1.35	2.35	1.58
NB4-BCT	62.6	1.75	1.49	3.08	1.29
NB6-MD1	35.5	7.79	14.58	4.85	12.30
NB6-NSC	81.0	3.15	2.97	4.04	3.25
RG1-HDM	17.6	1.24	1.47	0.54	1.21
RG1-MD1	24.0	4.13	9.02	2.30	5.30
RG1-NSC	73.6	1.70	3.44	1.19	2.01
RG1-UCT	57.0	2.21	3.15	2.28	3.75
RG2-BCT	62.5	0.71	1.55	0.34	0.95
RG4-BCT	62.5	0.37	0.21	0.49	0.19
RG4-HDM	17.7	2.10	2.40	0.77	1.09
RG4-UCT	57.0	1.56	3.21	0.84	3.51
RG4-WES	155.0	1.96	1.78	2.55	2.02
RG5-HDM	17.7	0.42	0.71	0.15	0.47
RG5-MD1	24.2	1.72	5.26	0.98	1.91
RG5-NSC	74.0	0.73	1.71	0.65	1.40

Average Rg/Lg(AV) Ratio = 2.50
Average Rg/Lg(AV) Ratio (for Distances > 50 km) = 1.58

TABLE 4

Rg/Lg AND Rg/P RATIOS FOR EARTHQUAKES

Event-Station	Distance (km)	Rg/Lg(AV)	Rg/P(AV)	Rg/Lg(MAX)	Rg/P(MAX)
ARDF-BCT	62.5	0.11	0.55	0.05	0.68
ARDF-ECT	99.6	0.13	0.42	0.09	0.33
ARDF-MD3	124.3	0.27	0.46	0.25	0.35
ARDA-BCT	63.7	0.19	0.83	0.14	1.29
ARDA-ECT	100.8	0.10	0.43	0.12	0.60
ARDA-MD3	129.0	0.13	0.20	0.21	0.16
BXBR-MD1	136.2	0.95	3.03	1.02	3.69
BXBR-MD3	140.5	0.67	1.47	0.72	1.15
BXBR-NSC	120.6	0.93	2.66	1.23	3.82
BXBR-QUA	74.6	1.05	2.30	2.26	1.44
BXBR-UCT	100.6	0.72	1.38	0.58	1.19
ERVG-HDM	123.1	0.12	0.28	0.14	0.29
ERVG-MD1	115.3	0.33	0.76	0.25	0.44
ERVG-NSC	131.3	0.19	0.34	0.08	0.09
ERVG-UCT	85.1	0.17	0.53	0.14	0.17
ERVG-WES	91.2	0.33	0.89	0.33	1.02
MDUS-BCT	87.0	0.39	1.55	0.50	2.26
MDUS-NSC	50.0	2.34	11.5	2.42	7.83
MDUS-QUA	103.0	0.58	1.19	0.56	0.83
MDUS-WES	133.0	0.43	1.45	0.26	0.88

TABLE 5

ESTIMATING DEPTH FROM Rg/Lg RATIOS

Event(s)	Depth (km)	Average Rg/Lg Ratio r(h)	Normalized r(h) $r_n(h)$	Depth (from Rg/Lg)
Ardsley, NY Earthquakes	*5.2	0.16	0.10	--
Moodus, CT Earthquake	*1.6	0.93	0.59	--
Boxboro, MA Earthquake	?	0.86	0.54	1.2
Erving, MA Earthquake	?	0.22	0.14	3.0
Blasts $50 \leq x \leq 170$ km	0.0	1.58	1.00	--

* from aftershock survey
x = distance

FIGURE CAPTIONS

FIGURE 1: (a) Stations of the New England Seismic Network (NESN) operated by Weston Observatory. (b) Approximate amplitude response curve for the NESN stations. Most of the stations are operated with gains of either ~100 or ~200 counts/micron at 1 Hz. (c) Stations of the Moodus, CT seismic array

FIGURE 2: Examples of vertical component seismograms and spectra from this study. (a) North Branford, CT quarry blast recorded at station MD1, (b) Reed Gap, CT quarry blast recorded at station UCT, (c) Reed Gap, CT quarry blast recorded at station NSC, and (d) Ardsley, NY earthquake recorded at station BCT. These spectra (as well as the spectra from other events discussed in this paper) have not been corrected for instrument response because the instruments all have similar responses [Figure 1(b)] that enhance the frequency range of the signals.

FIGURE 3: (a) Models of the shallow crust in New England. CHB is the Chiburis et al. (1977) refraction model of southern New England. EH is the Eastern Highlands model of Kafka and Dollin (1985) determined from trial-and-error fitting of Rg dispersion data in southern New England. BADR is the model of Kafka and Reiter (1988) determined from linearized inversion of Rg dispersion data in the "Bronson-Avalon" dispersion region in southern New England (see Kafka, 1988). (b) Displacement-depth eigenfunctions for vertical component of Rg waves calculated for the BADR crustal model shown in (a). These eigenfunctions were calculated using the method of Saito (1967).

FIGURE 4: (a) Narrow bandpass filter analysis of seismogram recorded from Reed Gap, CT quarry blast at station UCT. The seismogram is narrow bandpass filtered about a series of center frequencies, and the results are shown on the left as a

contour plot of group velocity vs. period. The vertical axis is amplitude; each unit of amplitude in this contour plot represents a difference of 2 db. Shaded areas indicate highest amplitudes. (b) Narrow bandpass filter analysis of seismogram recorded from North Branford, CT quarry blast at station MD1. (c) Narrow bandpass filter analysis of seismogram recorded from Ardsley, NY earthquake at station BCT.

FIGURE 5: (a) Narrow bandpass filter analysis of seismogram from the Erving, MA earthquake recorded at station WES. On the left is a plot of group velocity vs. period. The vertical axis is amplitude; each unit of amplitude in the contour plot represents a difference of 2 db. Shaded areas indicate highest amplitudes. (b) Mean and standard deviation of Rg group velocities for paths contained within three different dispersion regions in southern New England. These statistics are summarized in Kafka (1988). (c) Illustration of method of calculating Rg/Lg and Rg/P ratios from narrow bandpass filter analysis. U is group velocity in km/sec, and T is period in sec.

FIGURE 6: Histograms of log of Rg/Lg and Rg/P ratios for quarry blasts and for the Ardsley, NY earthquakes. (a) and (b): Ratios determined from calculating the average amplitude in the arrival time - frequency windows appropriate for each specific phase. (c) and (d): Ratios determined from calculating the maximum amplitude in the arrival time - frequency windows appropriate for each specific phase.

FIGURE 7: Histograms of log of Rg/Lg ratios for (a) quarry blasts and for (b) the Moodus, CT earthquake; (c) the Erving, MA earthquake; and (d) the Boxboro, MA earthquake. These ratios were determined from calculating the average amplitude in the arrival time - frequency windows appropriate for each specific phase.

FIGURE 8: Seismograms of (a) two of the largest quarry blasts recorded in southern New England @ 155 and 168 km, and (b) the Boxboro, MA earthquake showing clearly recorded Rg waves.

FIGURE 9: (a) Histogram of distances for (a) earthquakes in this study and for (b) blasts in this study. (c) Rg/Lg ratio as a function of distance from the source for blasts in this study. Also shown is a least-squares regression line and the corresponding correlation coefficient (r). (d) Same as (c) but excluding distances less than 50 km.

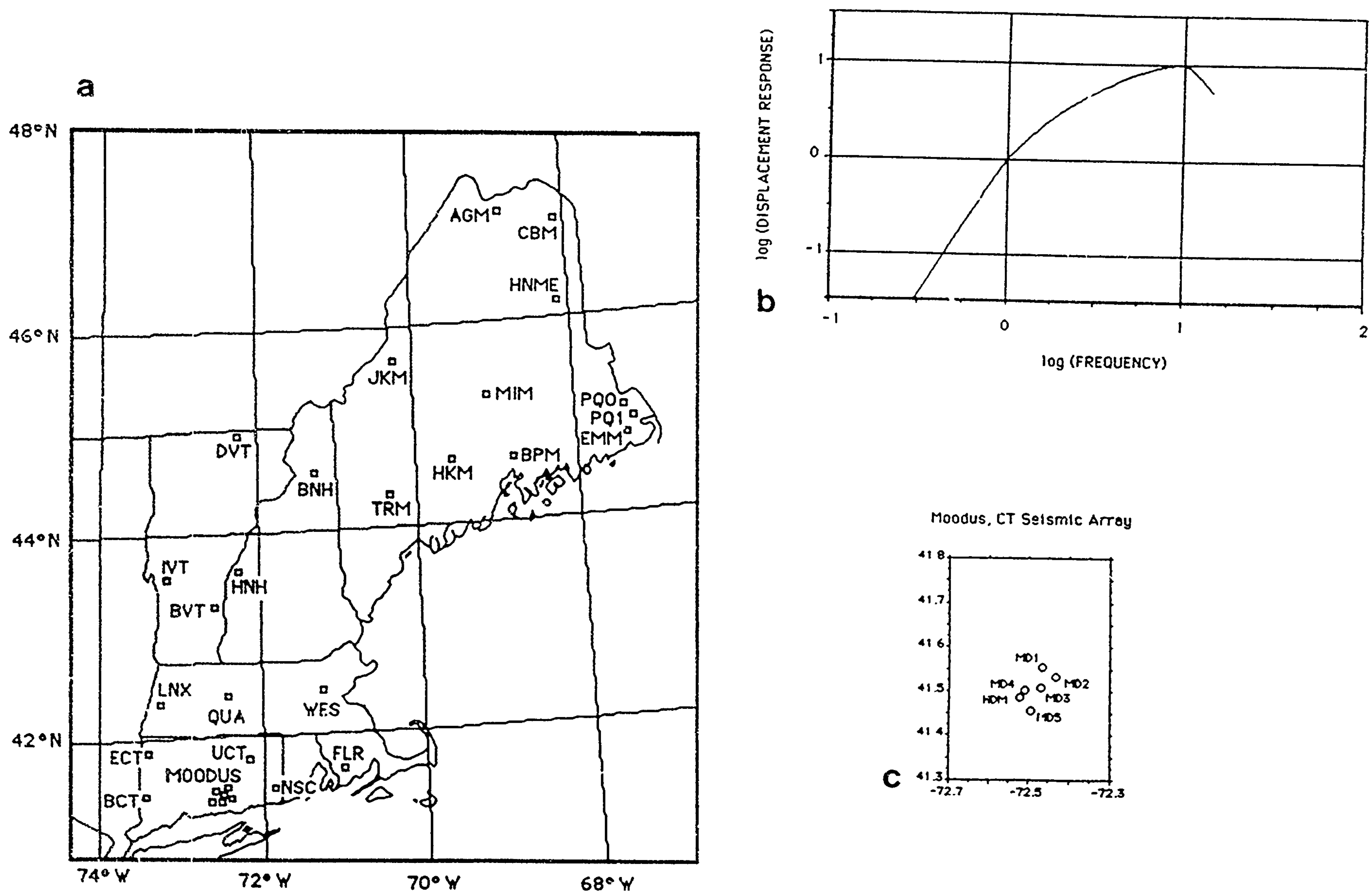
a
48° N
46° N
44° N
42° N
74° W
72° W
70° W
68° W
AGM
CBM
HNME
JKM
MIM
PQO
PQ1
EMM
DVT
BPM
HKM
BNH
TRM
IVT
HNH
BVT
LNX
QUA
WES
ECT
UCT
MOODUS
FLR
BCT
NSC
b
log (DISPLACEMENT RESPONSE)
log (FREQUENCY)
1
0
-1
2
Moodus, CT Seismic Array
c
41.8
41.7
41.6
41.5
41.4
41.3
-72.7
-72.5
-72.3
MD1
MD2
MD3
MD4
MD5
HDM

FIGURE 1

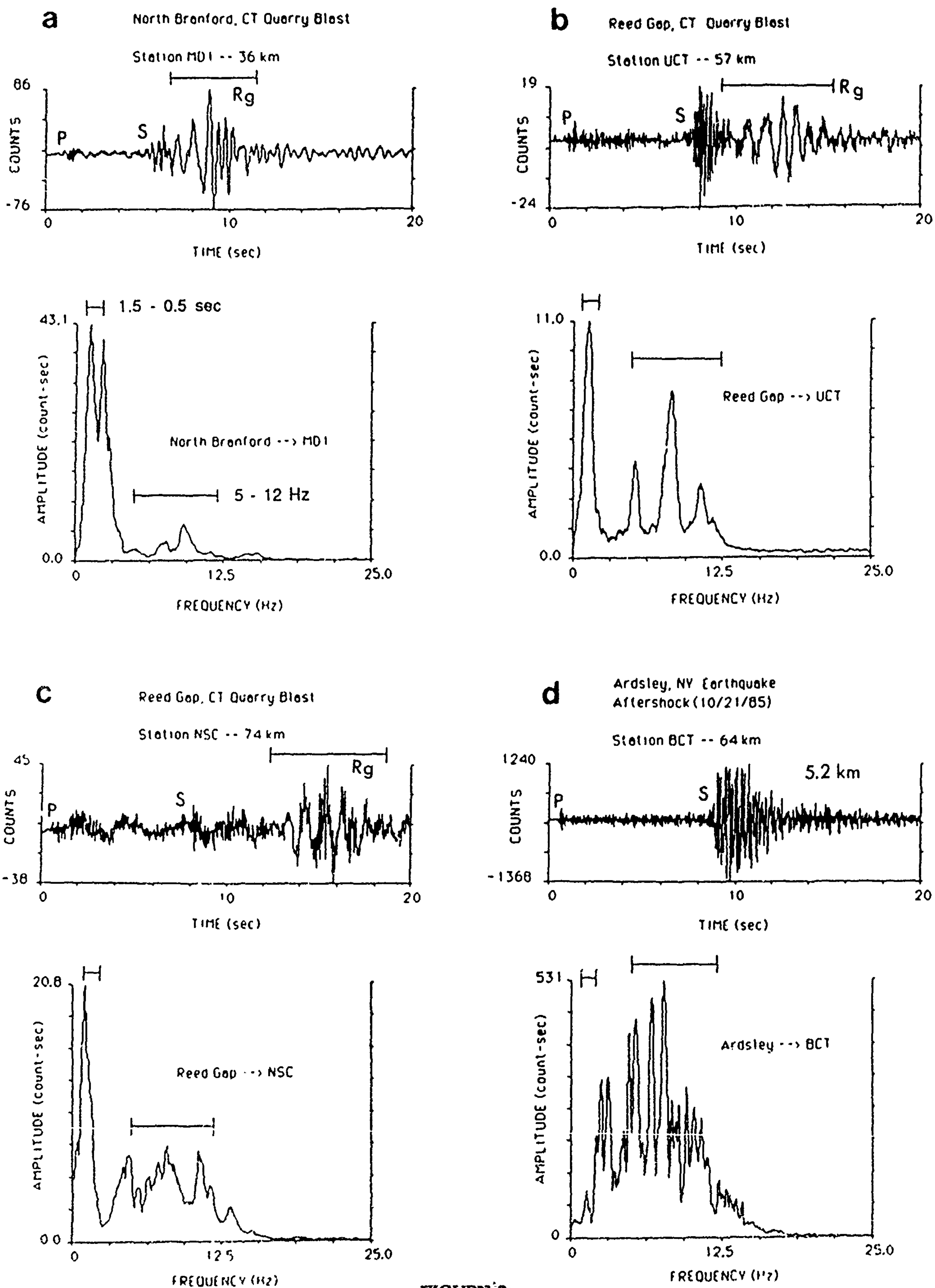

a
North Branford, CT Quarry Blast
Station MD1 -- 36 km
Rg
P
S
COUNTS
86
-76
0
10
20
TIME (sec)
1.5 - 0.5 sec
43.1
0.0
AMPLITUDE (count-sec)
North Branford --> MD1
5 - 12 Hz
0
12.5
25.0
FREQUENCY (Hz)
b
Reed Gap, CT Quarry Blast
Station UCT -- 57 km
Rg
P
S
19
-24
COUNTS
0
10
20
TIME (sec)
11.0
0.0
AMPLITUDE (count-sec)
Reed Gap --> UCT
0
12.5
25.0
FREQUENCY (Hz)
c
Reed Gap, CT Quarry Blast
Station NSC -- 74 km
Rg
45
-38
P
S
COUNTS
0
10
20
TIME (sec)
20.8
0.0
AMPLITUDE (count-sec)
Reed Gap --> NSC
0
12.5
25.0
FREQUENCY (Hz)
d
Ardsley, NY Earthquake
Aftershock (10/21/85)
Station BCT -- 64 km
5.2 km
1240
-1368
P
S
COUNTS
0
10
20
TIME (sec)
531
0
AMPLITUDE (count-sec)
Ardsley --> BCT
0
12.5
25.0
FREQUENCY (Hz)

FIGURE 2

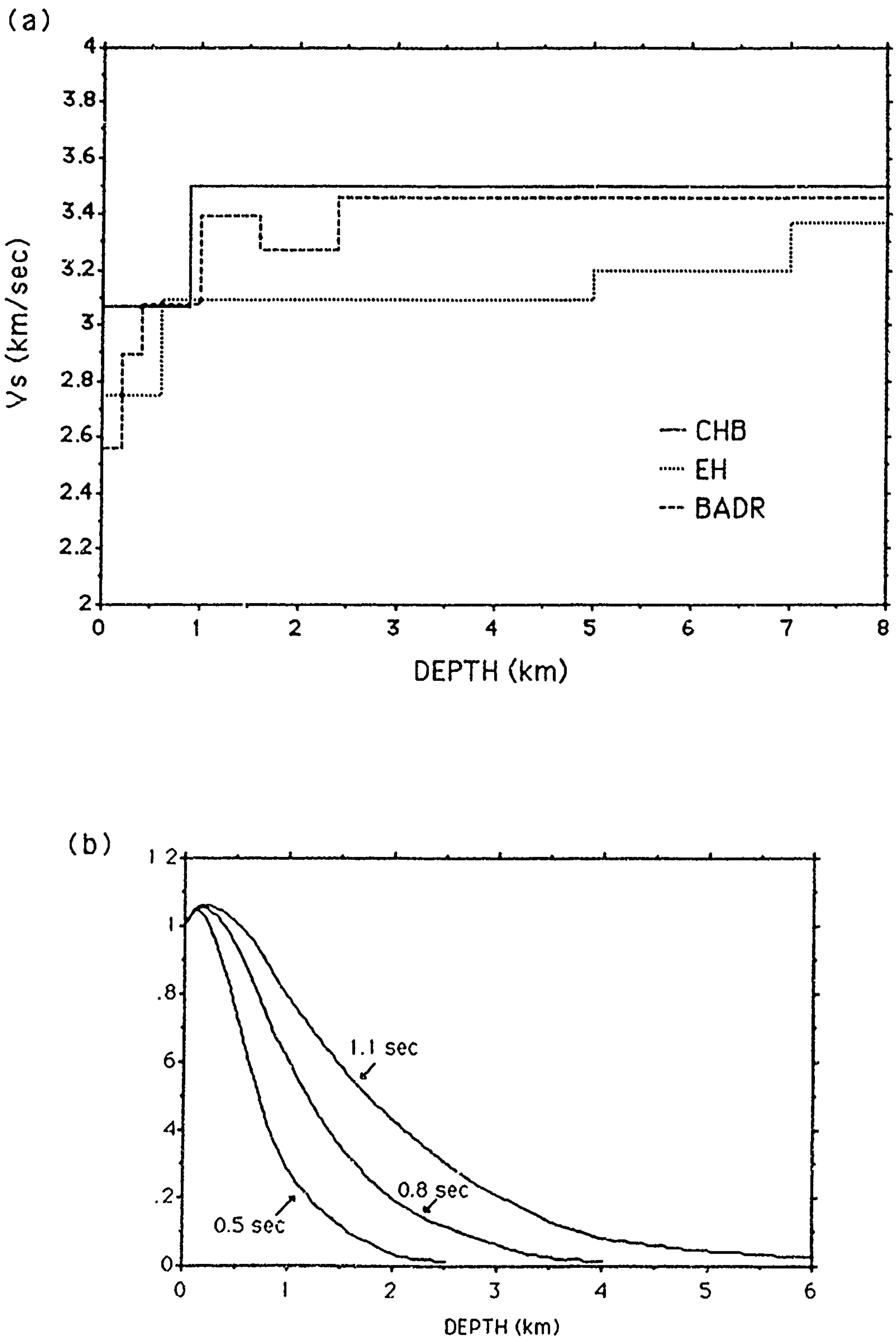

FIGURE 3

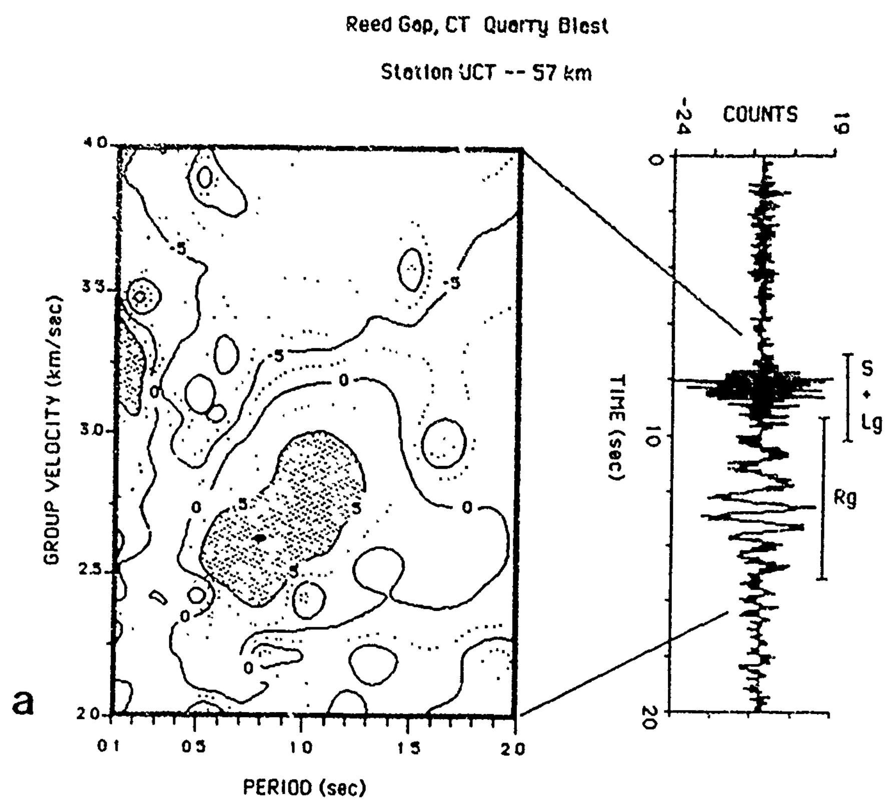
Reed Gap, CT Quarry Blast
Station UCT -- 57 km
GROUP VELOCITY (km/sec)
PERIOD (sec)
COUNTS
TIME (sec)
S + Lg
Rg
a

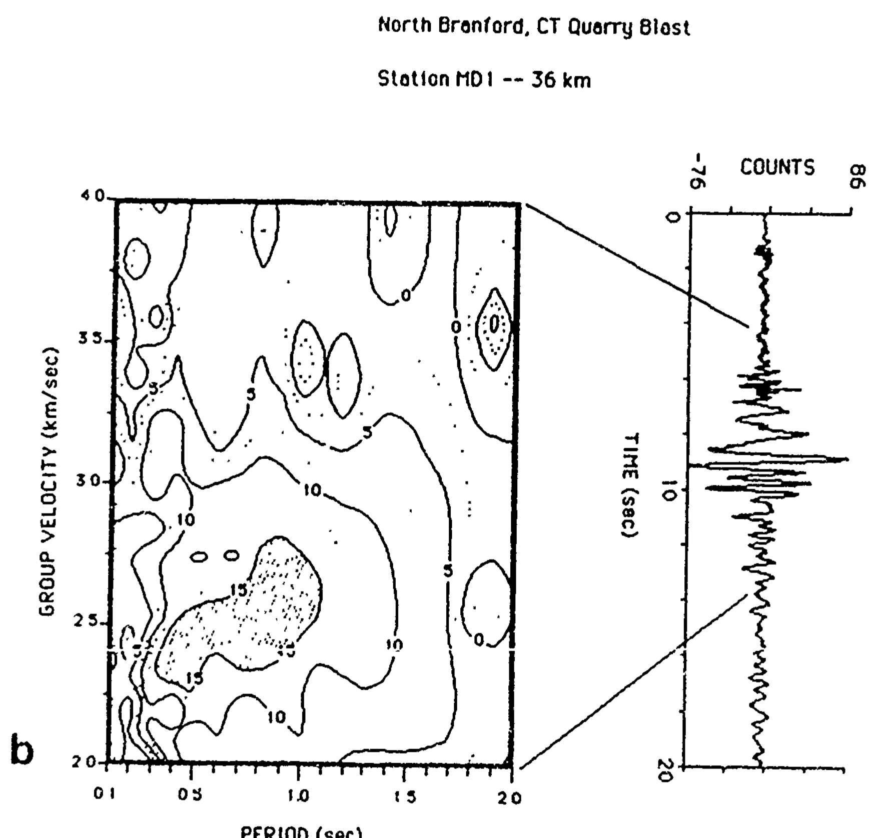
North Branford, CT Quarry Blast
Station MD1 -- 36 km
GROUP VELOCITY (km/sec)
PERIOD (sec)
COUNTS
TIME (sec)
b

FIGURE 4 (a, b)

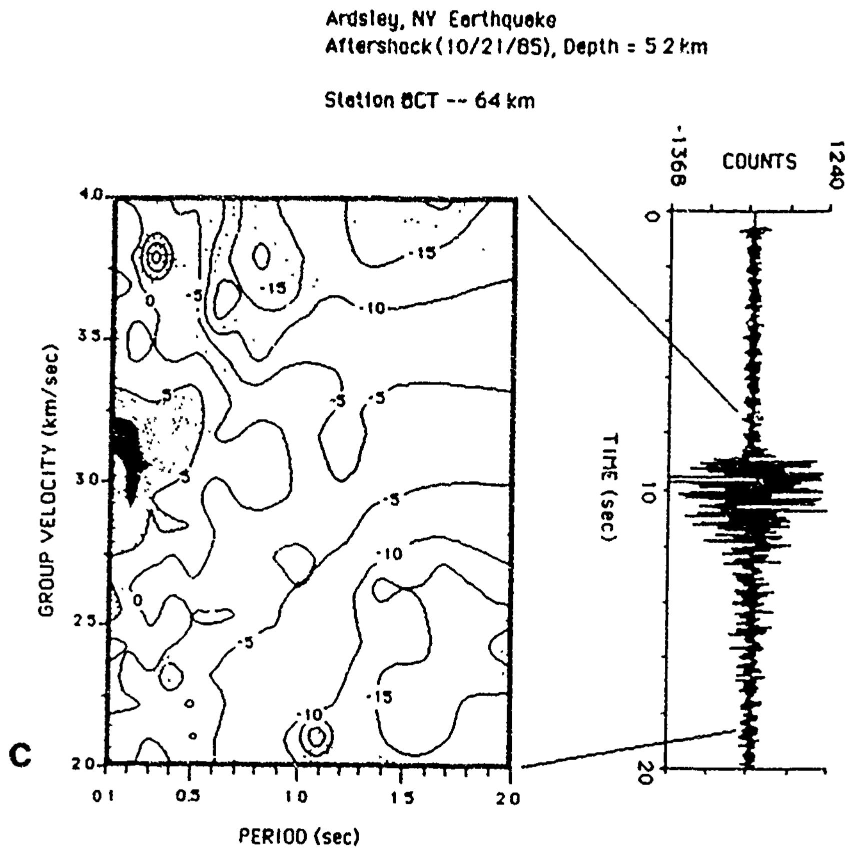
Ardsley, NY Earthquake
Aftershock (10/21/85), Depth = 5.2 km
Station BCT -- 64 km
GROUP VELOCITY (km/sec)
PERIOD (sec)
COUNTS
-1368
1240
TIME (sec)
C

FIGURE 4 (c)

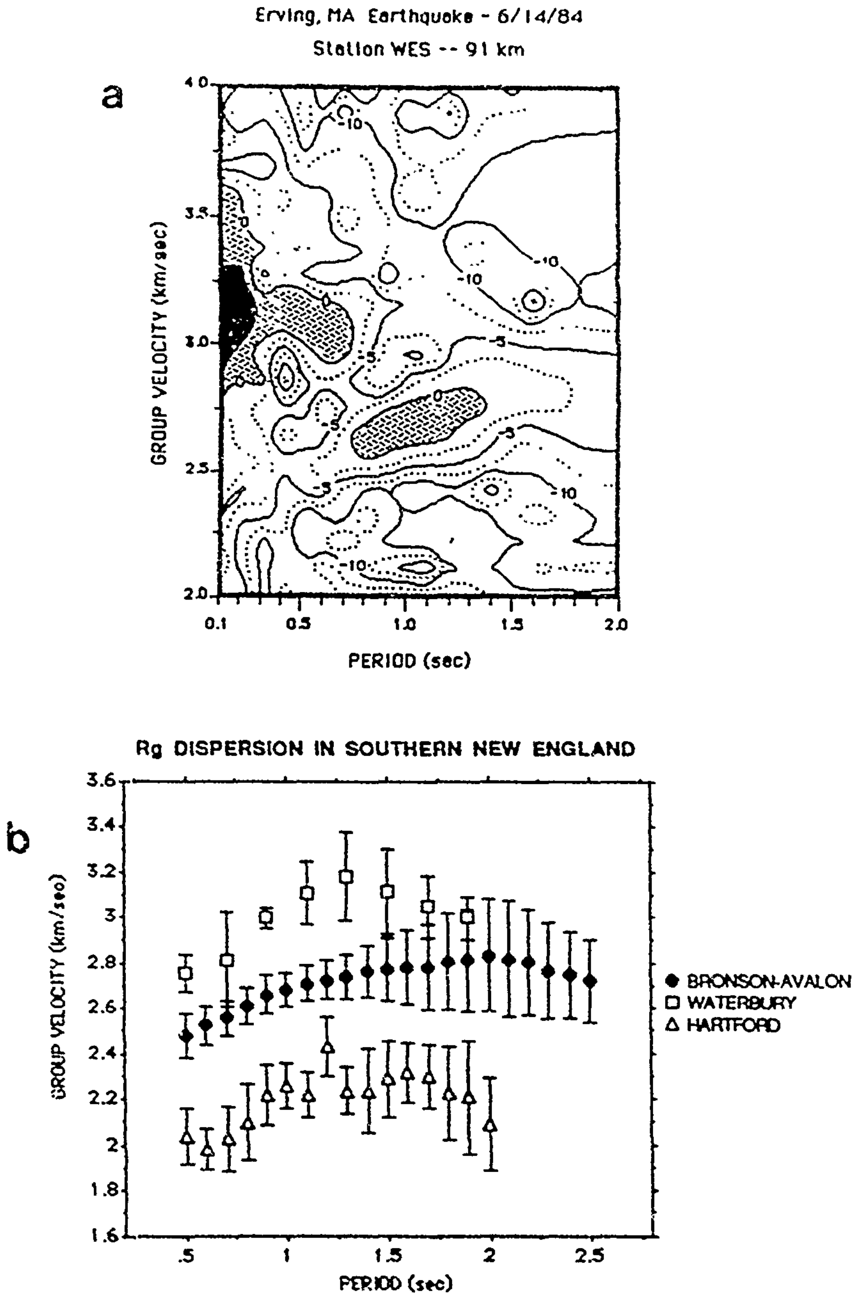

c

T →

U ↑

	0.1	0.3	0.5	0.7	0.9	1.1
6.6						
6.5	P	P				
6.4	P	P				
6.3	P	P				
6.2	P	P				
6.1	P	P				
6.0	P	P				
5.9	P	P				
5.8	P	P				
5.7	P	P				
5.6	P	P				
5.5	P	P				
5.4	P	P				
5.3	P	P				
5.2	P	P				
5.1	P	P				
5.0	P	P				
4.9	P	F				
4.8	P	F				
4.7	P	P				
4.6	F	P				
4.5	P	P				
4.4						
4.3						
4.2						
4.1						
4.0						
3.9						
3.8						
3.7	Lg	Lg				
3.6	Lg	Lg				
3.5	Lg	Lg				
3.4	Lg	Lg				
3.3	Lg	Lg				Rg
3.2	Lg	Lg				Rg
3.1	Lg	Lg		Rg	Rg	Rg
3.0				Rg	Rg	Rg
2.9			Rg	Rg	Rg	Rg
2.8			Rg	Rg	Rg	Rg
2.7			Rg	Rg	Rg	Rg
2.6			Rg	Rg	Rg	Rg
2.5			Rg	Rg	Rg	Rg
2.4			Rg	Rg	Rg	
2.3			Rg	Rg		
2.2			Rg			
2.1						
2.0						

FIGURE 5

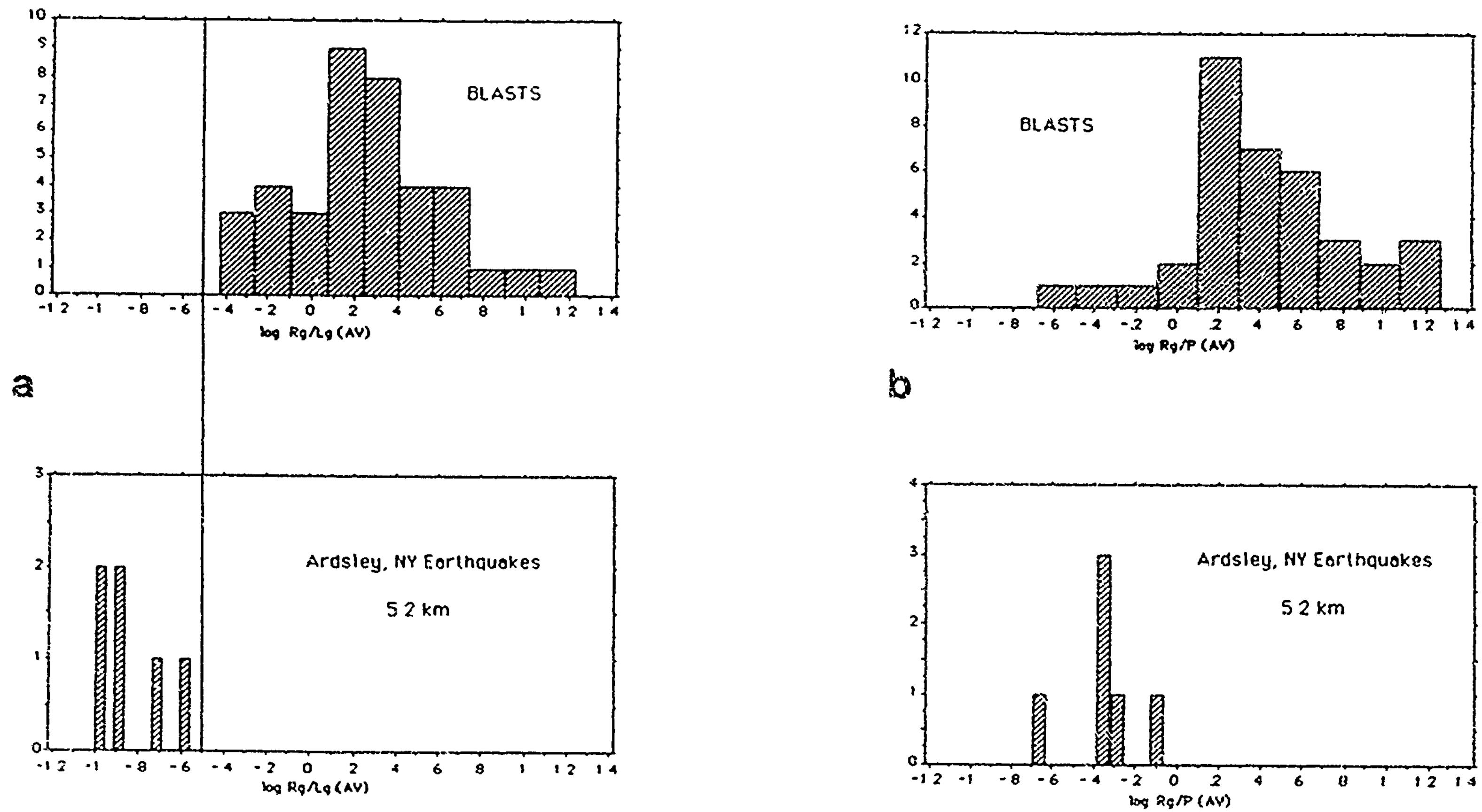
BLASTS
log Rg/Lg (AV)
Ardsley, NY Earthquakes
5 2 km
log Rg/Lg (AV)
a
BLASTS
log Rg/P (AV)
b
Ardsley, NY Earthquakes
5 2 km
log Rg/P (AV)

FIGURE 6 (a , b)

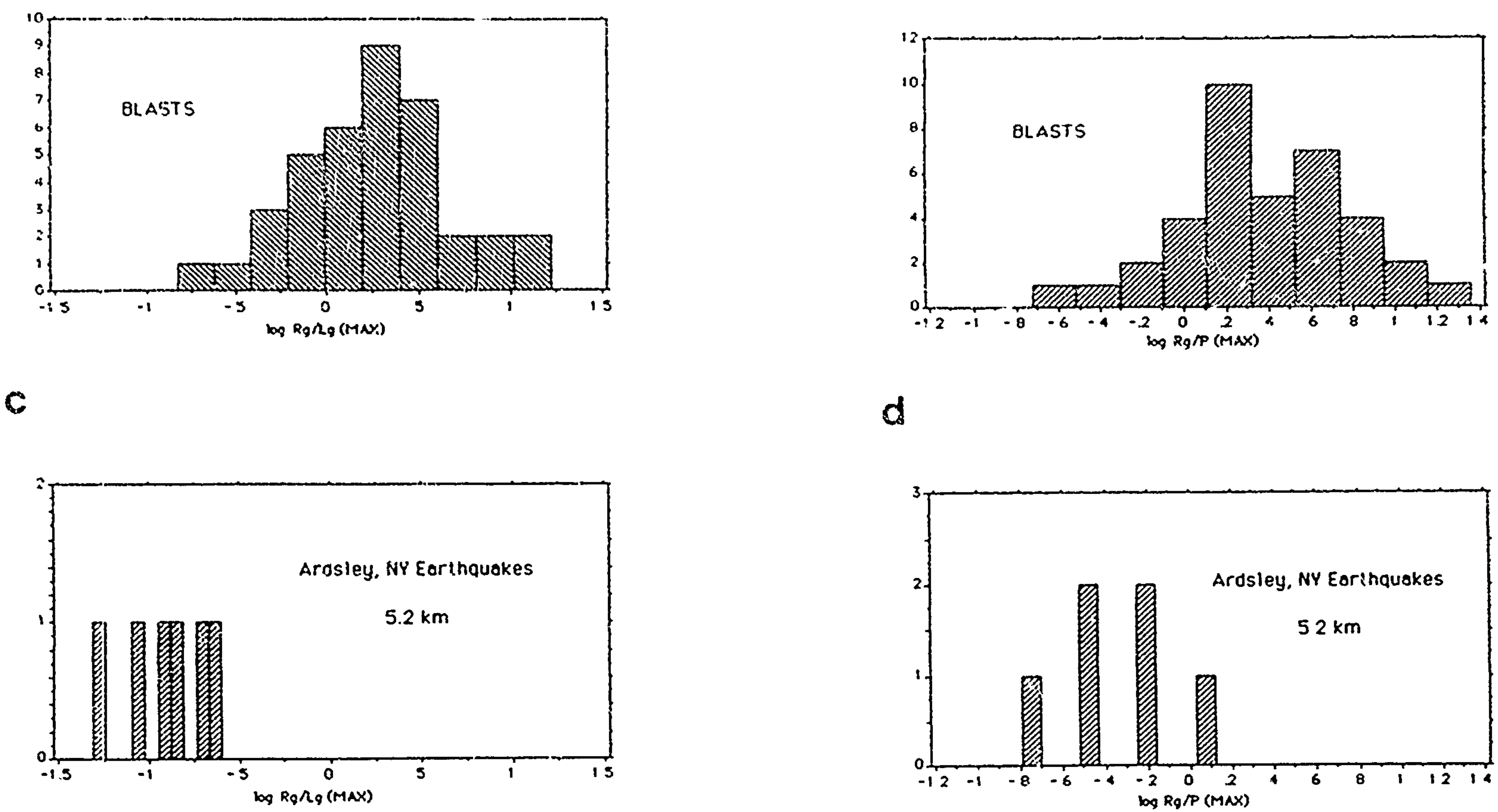

BLASTS
log Rg/Lg (MAX)
BLASTS
log Rg/P (MAX)
c
d
Ardsley, NY Earthquakes
5.2 km
log Rg/Lg (MAX)
Ardsley, NY Earthquakes
5 2 km
log Rg/P (MAX)

FIGURE 6 (c , d)

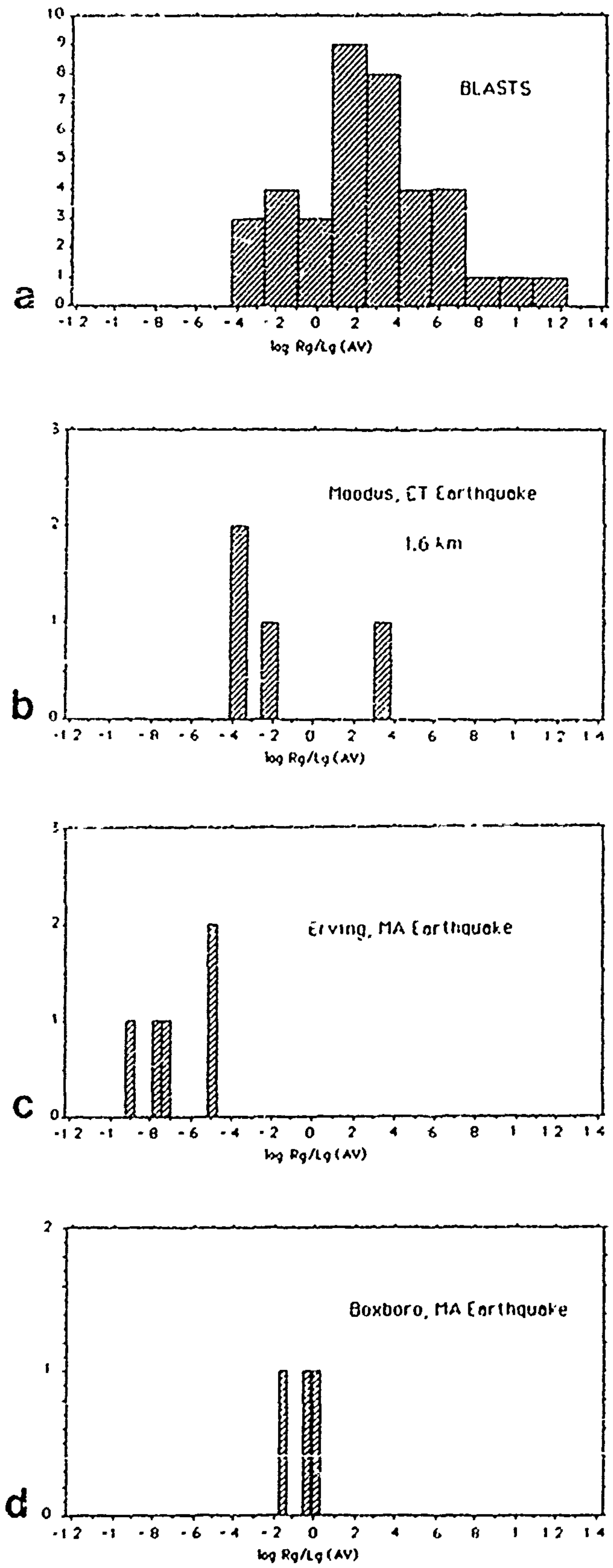
a
BLASTS
log Rg/Lg (AV)
b
Moodus, CT Earthquake
1.6 km
log Rg/Lg (AV)
c
Erving, MA Earthquake
log Rg/Lg (AV)
d
Boxboro, MA Earthquake
log Rg/Lg (AV)

FIGURE 7

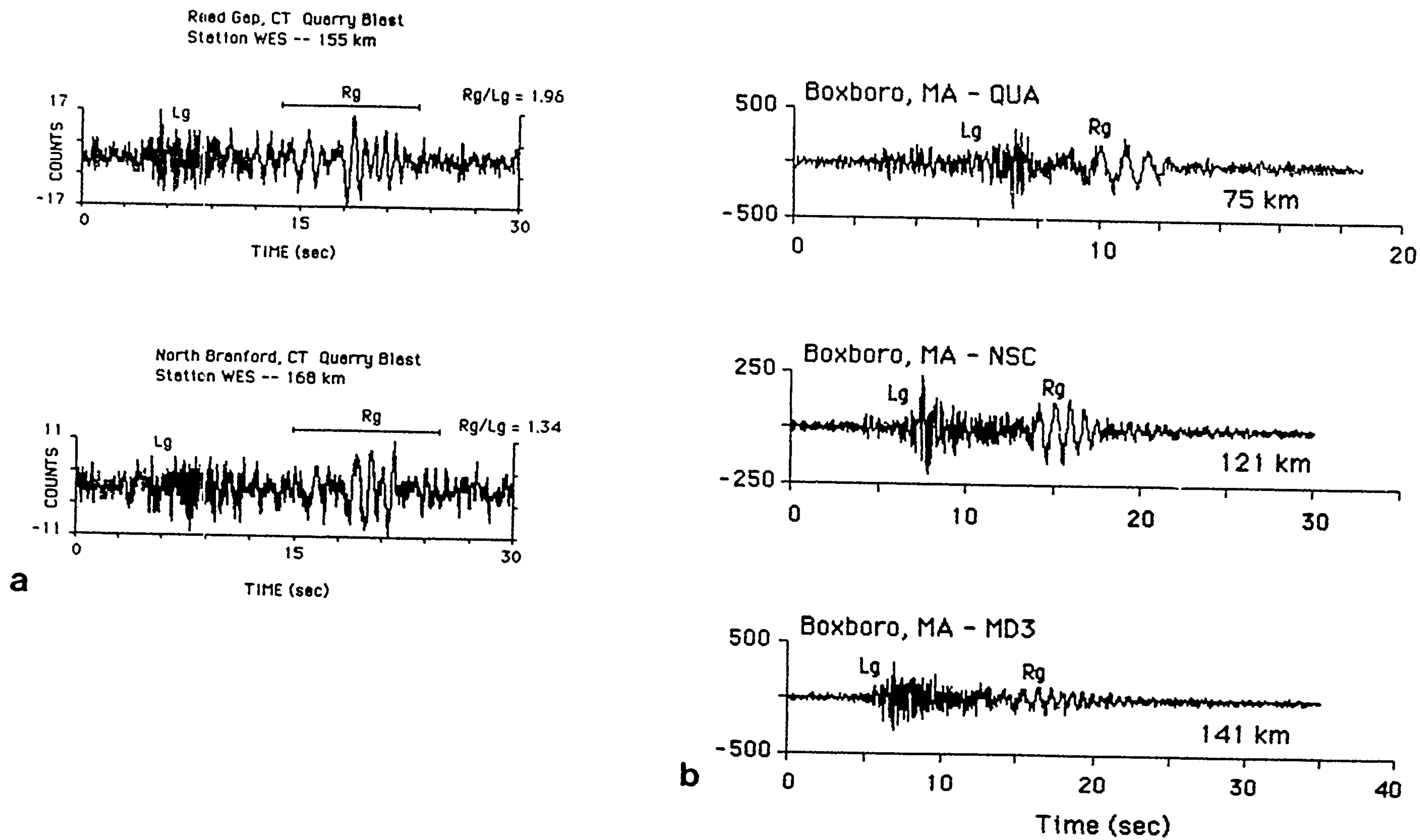
Reed Gap, CT Quarry Blast
Station WES -- 155 km
17
-17
COUNTS
Lg
Rg
Rg/Lg = 1.96
0
15
30
TIME (sec)
North Branford, CT Quarry Blast
Station WES -- 168 km
11
-11
COUNTS
Lg
Rg
Rg/Lg = 1.34
0
15
30
TIME (sec)
a
Boxboro, MA - QUA
500
-500
Lg
Rg
75 km
0
10
20
Boxboro, MA - NSC
250
-250
Lg
Rg
121 km
0
10
20
30
Boxboro, MA - MD3
500
-500
Lg
Rg
141 km
b
0
10
20
30
40
Time (sec)

FIGURE 8

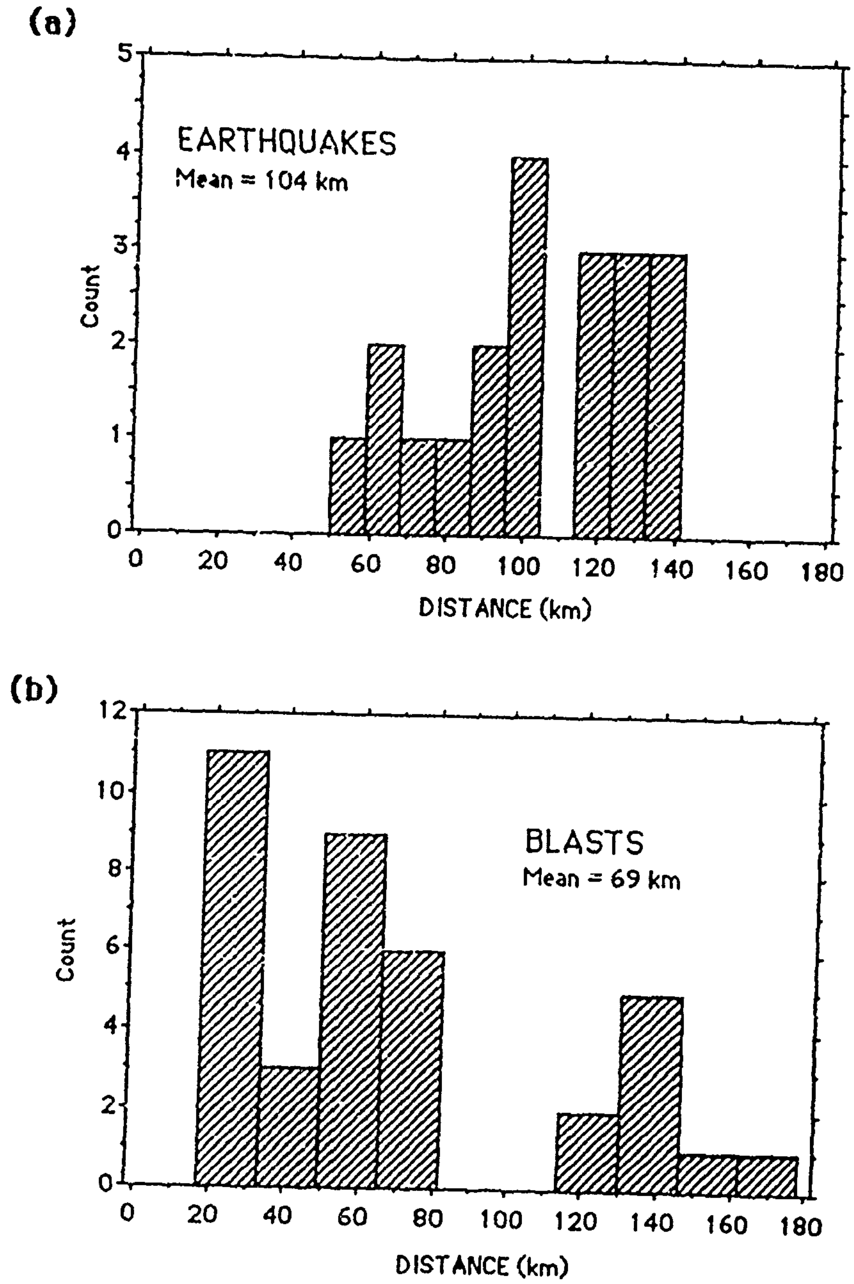
(a)
EARTHQUAKES
Mean = 104 km
Count
DISTANCE (km)
(b)
BLASTS
Mean = 69 km
Count
DISTANCE (km)

FIGURE 9 (a, b)

(c)

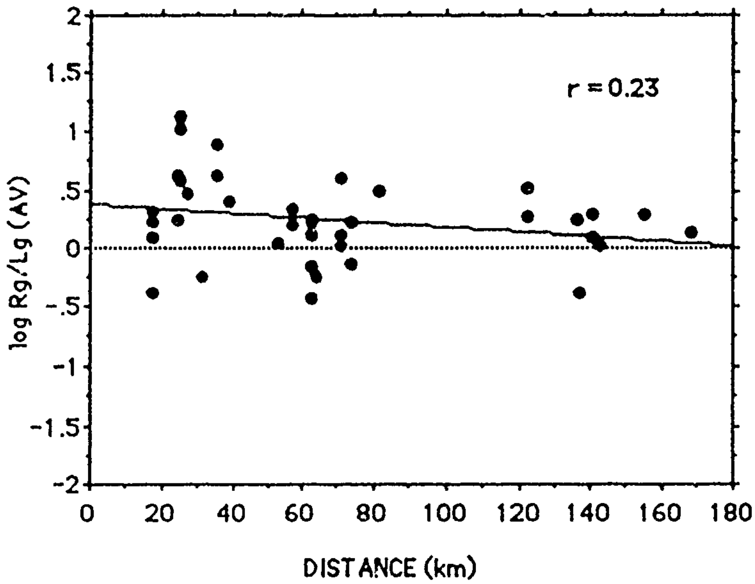

(d)

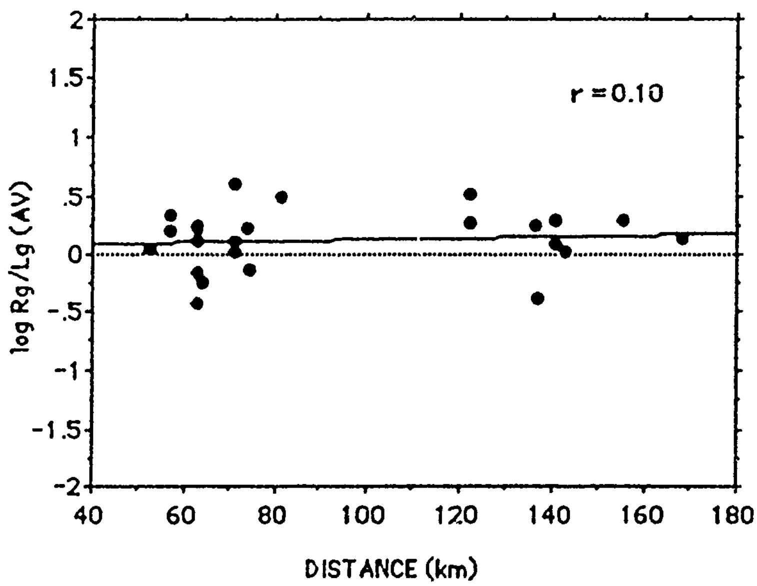

FIGURE 9 (c , d)

Prof. Thomas Ahrens
Seismological Lab, 252-21
Division of Geological & Planetary Sciences
California Institute of Technology
Pasadena, CA 91125

Prof. Charles B. Archambeau
CIRES
University of Colorado
Boulder, CO 80309

Prof. Muawia Barazangi
Institute for the Study of the Continent
Cornell University
Ithaca, NY 14853

Dr. Douglas R. Baumgardt
ENSCO, Inc
5400 Port Royal Road
Springfield, VA 22151-2388

Prof. Jonathan Berger
IGPP, A-025
Scripps Institution of Oceanography
University of California, San Diego
La Jolla, CA 92093

Dr. Lawrence J. Burdick
Woodward-Clyde Consultants
566 El Dorado Street
Pasadena, CA 91109-3245

Dr. Karl Coyner
New England Research, Inc.
76 Olcott Drive
White River Junction, VT 05001

Prof. Vernon F. Cormier
Department of Geology & Geophysics
U-45, Room 207
The University of Connecticut
Storrs, CT 06268

Professor Anton W. Dainty
Earth Resources Laboratory
Massachusetts Institute of Technology
42 Carleton Street
Cambridge, MA 02142

Prof. Steven Day
Department of Geological Sciences
San Diego State University
San Diego, CA 92182

Dr. Zoltan A. Der
ENSCO, Inc.
5400 Port Royal Road
Springfield, VA 22151-2388

Prof. John Ferguson
Center for Lithospheric Studies
The University of Texas at Dallas
P.O. Box 830688
Richardson, TX 75083-0688

Prof. Stanley Flatte
Applied Sciences Building
University of California
Santa Cruz, CA 95064

Dr. Alexander Florence
SRI International
333 Ravenswood Avenue
Menlo Park, CA 94025-3493

Prof. Henry L. Gray
Vice Provost and Dean
Department of Statistical Sciences
Southern Methodist University
Dallas, TX 75275

Dr. Indra Gupta
Teledyne Geotech
314 Montgomery Street
Alexandria, VA 22314

Prof. David G. Harkrider
Seismological Laboratory
Division of Geological & Planetary Sciences
California Institute of Technology
Pasadena, CA 91125

Prof. Donald V. Helmberger
Seismological Laboratory
Division of Geological & Planetary Sciences
California Institute of Technology
Pasadena, CA 91125

Prof. Eugene Herrin
Institute for the Study of Earth and Man
GeophysicalLaboratory
Southern Methodist University
Dallas, TX 75275

Prof . Robert B. Herrmann
Department of Earth & Atmospheric Sciences
St. Louis University
St. Louis, MO 63156

Prof. Bryan Isacks
Cornell University
Department of Geological Sciences
SNEE Hall
Ithaca, NY 14850

Dr. Rong-Song Jih
Teledyne Geotech
314 Montgomery Street
Alexandria, VA 22314

Prof. Lane R. Johnson
Seismographic Station
University of California
Berkeley, CA 94720

Prof. Alan Kafka
Department of Geology & Geophysics
Boston College
Chestnut Hill, MA 02167

Dr. Richard LaCoss
MIT-Lincoln Laboratory
M-200B
P. O. Box 73
Lexington, MA 02173-0073 (3 copies)

Prof Fred K. Lamb
University of Illinois at Urbana-Champaign
Department of Physics
1110 West Green Street
Urbana, IL 61801

Prof. Charles A. Langston
Geosciences Department
403 Deike Building
The Pennsylvania State University
University Park, PA 16802

Prof. Thorne Lay
Institute of Tectonics
Earth Science Board
University of California, Santa Cruz
Santa Cruz, CA 95064

Prof. Arthur Lerner-Lam
Lamont-Doherty Geological Observatory
of Columbia University
Palisades, NY 10964

Dr. Christopher Lynnes
Teledyne Geotech
314 Montgomery Street
Alexandria, VA 22314

Prof. Peter Malin
University of California at Santa Barbara
Institute for Crustal Studies
Santa Barbara, CA 93106

Dr. Randolph Martin, III
New England Research, Inc.
76 Olcott Drive
White River Junction, VT 05001

Dr. Gary McCartor
Mission Research Corporation
735 State Street
P.O. Drawer 719
Santa Barbara, CA 93102 (2 copies)

Prof. Thomas V. McEvilly
Seismographic Station
University of California
Berkeley, CA 94720

Dr. Keith L. McLaughlin
S-CUBED
A Division of Maxwell Laboratory
P.O. Box 1620
La Jolla, CA 92038-1620

Prof. William Menke
Lamont-Doherty Geological Observatory
of Columbia University
Palisades, NY 10964

Stephen Miller
SRI International
333 Ravenswood Avenue
Box AF 116
Menlo Park, CA 94025-3493

Prof. Bernard Minster
IGPP, A-025
Scripps Institute of Oceanography
University of California, San Diego
La Jolla, CA 92093

Prof. Brian J. Mitchell
Department of Earth & Atmospheric Sciences
St. Louis University
St. Louis, MO 63156

Mr. Jack Murphy
S-CUBED, A Division of Maxwell Laboratory
11800 Sunrise Valley Drive
Suite 1212
Reston, VA 22091 (2 copies)

Dr. Bao Nguyen
GL/LWH
Hanscom AFB, MA 01731-5000

Prof. John A. Orcutt
IGPP, A-025
Scripps Institute of Oceanography
University of California, San Diego
La Jolla, CA 92093

Prof. Keith Priestley
University of Cambridge
Bullard Labs., Dept. of Earth Sciences
Madingley Rise, Madingley Rd.
Cambridge CB3 OEZ, ENGLAND

Prof. Paul G. Richards
L-210
Lawrence Livermore National Laboratory
Livermore, CA 94550

Dr. Wilmer Rivers
Teledyne Geotech
314 Montgomery Street
Alexandria, VA 22314

Prof. Charles G. Sammis
Center for Earth Sciences
University of Southern California
University Park
Los Angeles, CA 90089-0741

Prof. Christopher H. Scholz
Lamont-Doherty Geological Observatory
of Columbia University
Palisades, NY 10964

Prof. David G. Simpson
Lamont-Doherty Geological Observatory
of Columbia University
Palisades, NY 10964

Dr. Jeffrey Stevens
S-CUBED
A Division of Maxwell Laboratory
P.O. Box 1620
La Jolla, CA 92038-1620

Prof. Brian Stump
Institute for the Study of Earth & Man
Geophysical Laboratory
Southern Methodist University
Dallas, TX 75275

Prof. Jeremiah Sullivan
University of Illinois at Urbana-Champaign
Department of Physics
1110 West Green Street
Urbana, IL 61801

Prof. Clifford Thurber
University of Wisconsin-Madison
Department of Geology & Geophysics
1215 West Dayton Street
Madison, WS 53706

Prof. M. Nafi Toksoz
Earth Resources Lab
Massachusetts Institute of Technology
42 Carleton Street
Cambridge, MA 02142

Prof. John E. Vidale
University of California at Santa Cruz
Seismological Laboratory
Santa Cruz, CA 95064

Prof. Terry C. Wallace
Department of Geosciences
Building #77
University of Arizona
Tucson, AZ 85721

Dr. Raymond Willeman
GL/LWH
Hanscom AFB, MA 01731-5000

Dr. Lorraine Wolf
GL/LWH
Hanscom AFB, MA 01731-5000

Prof. Francis T. Wu
Department of Geological Sciences
State University of New York
at Binghamton
Vestal, NY 13901

OTHERS (United States)

Dr. Monem Abdel-Gawad
Rockwell International Science Center
1049 Camino Dos Rios
Thousand Oaks, CA 91360

Prof. Keiiti Aki
Center for Earth Sciences
University of Southern California
University Park
Los Angeles, CA 90089-0741

Prof. Shelton S. Alexander
Geosciences Department
403 Deike Building
The Pennsylvania State University
University Park, PA 16802

Dr. Kenneth Anderson
BBNSTC
Mail Stop 14/1B
Cambridge, MA 02238

Dr. Ralph Archuleta
Department of Geological Sciences
University of California at Santa Barbara
Santa Barbara, CA 93102

Dr. Thomas C. Bache, Jr.
Science Applications Int'l Corp.
10210 Campus Point Drive
San Diego, CA 92121 (2 copies)

J. Barker
Department of Geological Sciences
State University of New York
at Binghamton
Vestal, NY 13901

Dr. T.J. Bennett
S-CUBED
A Division of Maxwell Laboratory
11800 Sunrise Valley Drive, Suite 1212
Reston, VA 22091

Mr. William J. Best
907 Westwood Drive
Vienna, VA 22180

Dr. N. Biswas
Geophysical Institute
University of Alaska
Fairbanks, AK 99701

Dr. G.A. Bollinger
Department of Geological Sciences
Virginia Polytechnical Institute
21044 Derring Hall
Blacksburg, VA 24061

Dr. Stephen Bratt
Science Applications Int'l Corp.
10210 Campus Point Drive
San Diego, CA 92121

Michael Browne
Teledyne Geotech
3401 Shiloh Road
Garland, TX 75041

Mr. Roy Burger
1221 Serry Road
Schenectady, NY 12309

Dr. Robert Burridge
Schlumberger-Doll Research Center
Old Quarry Road
Ridgefield, CT 06877

Dr. Jerry Carter
Rondout Associates
P.O. Box 224
Stone Ridge, NY 12484

Dr. W. Winston Chan
Teledyne Geotech
314 Montgomery Street
Alexandria, VA 22314-1581

Dr. Theodore Cherry
Science Horizons, Inc.
710 Encinitas Blvd., Suite 200
Encinitas, CA 92024 (2 copies)

Prof. Jon F. Claerbout
Department of Geophysics
Stanford University
Stanford, CA 94305

Prof. Robert W. Clayton
Seismological Laboratory
Division of Geological & Planetary Sciences
California Institute of Technology
Pasadena, CA 91125

Prof. F. A. Dahlen
Geological and Geophysical Sciences
Princeton University
Princeton, NJ 08544-0636

Prof. Adam Dziewonski
Hoffman Laboratory
Harvard University
20 Oxford St
Cambridge, MA 02138

Prof. John Ebel
Department of Geology & Geophysics
Boston College
Chestnut Hill, MA 02167

Eric Fielding
SNEE Hall
INSTOC
Cornell University
Ithaca, NY 14853

Prof. Donald Forsyth
Department of Geological Sciences
Brown University
Providence, RI 02912

Dr. Cliff Frolich
Institute of Geophysics
8701 North Mopac
Austin, TX 78759

Prof. Art Frankel
Mail Stop 922
Geological Survey
790 National Center
Reston, VA 22092

Dr. Anthony Gangi
Texas A&M University
Department of Geophysics
College Station, TX 77843

Dr. Freeman Gilbert
Inst. of Geophysics & Planetary Physics
University of California, San Diego
P.O. Box 109
La Jolla, CA 92037

Mr. Edward Giller
Pacific Sierra Research Corp.
1401 Wilson Boulevard
Arlington, VA 22209

Dr. Jeffrey W. Given
Sierra Geophysics
11255 Kirkland Way
Kirkland, WA 98033

Prof. Stephen Grand
University of Texas at Austin
Department of Geological Sciences
Austin, TX 78713-7909

Prof. Roy Greenfield
Geosciences Department
403 Deike Building
The Pennsylvania State University
University Park, PA 16802

Dan N. Hagedorn
Battelle
Pacific Northwest Laboratories
Battelle Boulevard
Richland, WA 99352

Kevin Hutchenson
Department of Earth Sciences
St. Louis University
3507 Laclede
St. Louis, MO 63103

Prof. Thomas H. Jordan
Department of Earth, Atmospheric
and Planetary Sciences
Massachusetts Institute of Technology
Cambridge, MA 02139

Robert C. Kemerait
ENSCO, Inc.
445 Pineda Court
Melbourne, FL 32940

William Kikendall
Teledyne Geotech
3401 Shiloh Road
Garland, TX 75041

Prof. Leon Knopoff
University of California
Institute of Geophysics & Planetary Physics
Los Angeles, CA 90024

Prof. L. Timothy Long
School of Geophysical Sciences
Georgia Institute of Technology
Atlanta, GA 30332

Prof. Art McGarr
Mail Stop 977
Geological Survey
345 Middlefield Rd.
Menlo Park, CA 94025

Dr. George Mellman
Sierra Geophysics
11255 Kirkland Way
Kirkland, WA 98033

Prof. John Nabelek
College of Oceanography
Oregon State University
Corvallis, OR 97331

Prof. Geza Nagy
University of California, San Diego
Department of Ames, M.S. B-010
La Jolla, CA 92093

Prof. Amos Nur
Department of Geophysics
Stanford University
Stanford, CA 94305

Prof. Jack Oliver
Department of Geology
Cornell University
Ithaca, NY 14850

Prof. Robert Phinney
Geological & Geophysical Sciences
Princeton University
Princeton, NJ 08544-0636

Dr. Paul Pomeroy
Rondout Associates
P.O. Box 224
Stone Ridge, NY 12484

Dr. Jay Pulli
RADIX System, Inc.
2 Taft Court, Suite 203
Rockville, MD 20850

Dr. Norton Rimer
S-CUBED
A Division of Maxwell Laboratory
P.O. Box 1620
La Jolla, CA 92038-1620

Prof. Larry J. Ruff
Department of Geological Sciences
1006 C.C. Little Building
University of Michigan
Ann Arbor, MI 48109-1063

Dr. Richard Sailor
TASC Inc.
55 Walkers Brook Drive
Reading, MA 01867

Thomas J. Sereno, Jr.
Science Application Int'l Corp.
10210 Campus Point Drive
San Diego, CA 92121

John Sherwin
Teledyne Geotech
3401 Shiloh Road
Garland, TX 75041

Prof. Robert Smith
Department of Geophysics
University of Utah
1400 East 2nd South
Salt Lake City, UT 84112

Prof. S. W. Smith
Geophysics Program
University of Washington
Seattle, WA 98195

Dr. Stewart Smith
IRIS Inc.
1616 North Fort Myer Drive
Suite 1440
Arlington, VA 22209

Dr. George Sutton
Rondout Associates
P.O. Box 224
Stone Ridge, NY 12484

Prof. L. Sykes
Lamont-Doherty Geological Observatory
of Columbia University
Palisades, NY 10964

Prof. Pradeep Talwani
Department of Geological Sciences
University of South Carolina
Columbia, SC 29208

Prof. Ta-liang Teng
Center for Earth Sciences
University of Southern California
University Park
Los Angeles, CA 90089-0741

Dr. R.B. Tittmann
Rockwell International Science Center
1049 Camino Dos Rios
P.O. Box 1085
Thousand Oaks, CA 91360

Dr. Gregory van der Vink
IRIS, Inc.
1616 North Fort Myer Drive
Suite 1440
Arlington, VA 22209

Professor Daniel Walker
University of Hawaii
Institute of Geophysics
Honolulu, HI 96822

William R. Walter
Seismological Laboratory
University of Nevada
Reno, NV 89557

Dr. Gregory Wojcik
Weidlinger Associates
4410 El Camino Real
Suite 110
Los Altos, CA 94022

Prof. John H. Woodhouse
Hoffman Laboratory
Harvard University
20 Oxford St.
Cambridge, MA 02138

Dr. Gregory B. Young
ENSCO, Inc.
5400 Port Royal Road
Springfield, VA 22151-2388

Dr. Ralph Alewine III
DARPA/NMRO
1400 Wilson Boulevard
Arlington, VA 22209-2308

Mr. James C. Battis
GL/LWH
Hanscom AFB, MA 01731-5000

Dr. Robert Blandford
DARPA/NMRO
1400 Wilson Boulevard
Arlington, VA 22209-2308

Eric Chael
Division 9241
Sandia Laboratory
Albuquerque, NM 87185

Dr. John J. Cipar
GL/LWH
Hanscom AFB, MA 01731-5000

Mr. Jeff Duncan
Office of Congressman Markey
2133 Rayburn House Bldg.
Washington, DC 20515

Dr. Jack Evernden
USGS - Earthquake Studies
345 Middlefield Road
Menlo Park, CA 94025

Art Frankel
USGS
922 National Center
Reston, VA 22092

Dr. T. Hanks
USGS
Nat'l Earthquake Research Center
345 Middlefield Road
Menlo Park, CA 94025

Dr. James Hannon
Lawrence Livermore Nat'l Laboratory
P.O. Box 808
Livermore, CA 94550

Paul Johnson
ESS-4, Mail Stop J979
Los Alamos National Laboratory
Los Alamos, NM 87545

Janet Johnston
GL/LWH
Hanscom AFB, MA 01731-5000

Dr. Katharine Kadinsky-Cade
GL/LWH
Hanscom AFB, MA 01731-5000

Ms. Ann Kerr
IGPP, A-025
Scripps Institute of Oceanography
University of California, San Diego
La Jolla, CA 92093

Dr. Max Koontz
US Dept of Energy/DP 5
Forrestal Building
1000 Independence Avenue
Washington, DC 20585

Dr. W.H.K. Lee
Office of Earthquakes, Volcanoes,
& Engineering
345 Middlefield Road
Menlo Park, CA 94025

Dr. William Leith
U.S. Geological Survey
Mail Stop 928
Reston, VA 22092

Dr. Richard Lewis
Director, Earthquake Engineering & Geophysics
U.S. Army Corps of Engineers
Box 631
Vicksburg, MS 39180

James F. Lewkowicz
GL/LWH
Hanscom AFB, MA 01731-5000

Mr. Alfred Lieberman
ACDA/VI-OA'State Department Bldg
Room 5726
320 - 21st Street, NW
Washington, DC 20451

Stephen Mangino
GL/LWH
Hanscom AFB, MA 01731-5000

Dr. Frank F. Pilotte
HQ AFTAC/TT
Patrick AFB, FL 32925-6001

Dr. Robert Masse
Box 25046, Mail Stop 967
Denver Federal Center
Denver, CO 80225

Katie Poley
CIA-OSWR/NED
Washington, DC 20505

Art McGarr
U.S. Geological Survey, MS-977
345 Middlefield Road
Menlo Park, CA 94025

Mr. Jack Rachlin
U.S. Geological Survey
Geology, Rm 3 C136
Mail Stop 928 National Center
Reston, VA 22092

Richard Morrow
ACDA/VI, Room 5741
320 21st Street N.W
Washington, DC 20451

Dr. Robert Reinke
WL/NTESG
Kirtland AFB, NM 87117-6008

Dr. Keith K. Nakanishi
Lawrence Livermore National Laboratory
P.O. Box 808, L-205
Livermore, CA 94550

Dr. Byron Ristvet
HQ DNA, Nevada Operations Office
Attn: NVCG
P.O. Box 98539
Las Vegas, NV 89193

Dr. Carl Newton
Los Alamos National Laboratory
P.O. Box 1663
Mail Stop C335, Group ESS-3
Los Alamos, NM 87545

Dr. George Rothe
HQ AFTAC/TGR
Patrick AFB, FL 32925-6001

Dr. Kenneth H. Olsen
Los Alamos Scientific Laboratory
P.O. Box 1663
Mail Stop C335, Group ESS-3
Los Alamos, NM 87545

Dr. Alan S. Ryall, Jr.
DARPA/NMRO
1400 Wilson Boulevard
Arlington, VA 22209-2308

Howard J. Patton
Lawrence Livermore National Laboratory
P.O. Box 808, L-205
Livermore, CA 94550

Dr. Michael Shore
Defense Nuclear Agency/SPSS
6801 Telegraph Road
Alexandria, VA 22310

Mr. Chris Paine
Office of Senator Kennedy
SR 315
United States Senate
Washington, DC 20510

Donald L. Springer
Lawrence Livermore National Laboratory
P.O. Box 808, L-205
Livermore, CA 94550

Colonel Jerry J. Perrizo
AFOSR/NP, Building 410
Bolling AFB
Washington, DC 20332-6448

Mr. Charles L. Taylor
GL/LWG
Hanscom AFB, MA 01731-5000

Dr. Thomas Weaver
Los Alamos National Laboratory
P.O. Box 1663, Mail Stop C335
Los Alamos, NM 87545

J.J. Zucca
Lawrence Livermore National Laboratory
Box 808
Livermore, CA 94550

GL/SULL
Research Library
Hanscom AFB , MA 01731-5000 (2 copies)

Secretary of the Air Force
(SAFRD)

Washington, DC 20330

Office of the Secretary Defense
DDR & E
Washington, DC 20330

HQ DNA
Attn: Technical Library
Washington, DC 20305

DARPA/RMO/RETRIEVAL
1400 Wilson Boulevard
Arlington, VA 22209

DARPA/RMO/Security Office
1400 Wilson Boulevard
Arlington, VA 22209

Geophysics Laboratory
Attn: XO
Hanscom AFB, MA 01731-5000

Geophysics Laboratory
Attn: LW
Hanscom AFB, MA 01731-5000

DARPA/PM
1400 Wilson Boulevard
Arlington, VA 22209

Defense Technical Information Center
Cameron Station
Alexandria, VA 22314 (5 copies)

Defense Intelligence Agency
Directorate for Scientific &
Technical Intelligence
Washington, DC 20301

AFTAC/CA
(STINFO)
Patrick AFB, FL 32925-6001

TACTEC
Battelle Memorial Institute
505 King Avenue
Columbus, OH 43201 (Final Report Only)

CONTRACTORS (Foreign)

Dr. Ramon Cabre, S.J.
Observatorio San Calixto
Casilla 5939
La Paz, Bolivia

Prof. Hans-Peter Harjes
Institute for Geophysik
Ruhr University/Bochum
P.O. Box 102148
4630 Bochum 1, FRG

Prof. Eystein Husebye
NTNF/NORSAR
P.O. Box 51
N-2007 Kjeller, NORWAY

Prof. Brian L.N. Kennett
Research School of Earth Sciences
Institute of Advanced Studies
G.P.O. Box 4
Canberra 2601, AUSTRALIA

Dr. Bernard Massinon
Societe Radiomana
27 rue Claude Bernard
75005 Paris, FRANCE (2 Copies)

Dr. Pierre Mecheler
Societe Radiomana
27 rue Claude Bernard
75005 Paris, FRANCE

Dr. Svein Mykkeltveit
NTNF/NORSAR
P.O. Box 51
N-2007 Kjeller, NORWAY

FOREIGN (Others)

Dr. Peter Basham
Earth Physics Branch
Geological Survey of Canada
1 Observatory Crescent
Ottawa, Ontario, CANADA K1A 0Y3

Dr. Eduard Berg
Institute of Geophysics
University of Hawaii
Honolulu, HI 96822

Dr. Michel Bouchon
I.R.I.G.M.-B.P. 68
38402 St. Martin D'Heres
Cedex, FRANCE

Dr. Hilmar Bungum
NTNF/NORSAR
P.O. Box 51
N-2007 Kjeller, NORWAY

Dr. Michel Campillo
Observatoire de Grenoble
I.R.I.G.M.-B.P. 53
38041 Grenoble, FRANCE

Dr. Kin Yip Chun
Geophysics Division
Physics Department
University of Toronto
Ontario, CANADA M5S 1A7

Dr. Alan Douglas
Ministry of Defense
Blacknest, Brimpton
Reading RG7-4RS, UNITED KINGDOM

Dr. Roger Hansen
NTNF/NORSAR
P.O. Box 51
N-2007 Kjeller, NORWAY

Dr. Manfred Henger
Federal Institute for Geosciences & Nat'l Res.
Postfach 510153
D-3000 Hanover 51, FRG

Ms. Eva Johannisson
Senior Research Officer
National Defense Research Inst.
P.O. Box 27322
S-102 54 Stockholm, SWEDEN

Dr. Fekadu Kebede
Seismological Section
Box 12019
S-750 Uppsala, SWEDEN

Dr. Tormod Kvaerna
NTNF/NORSAR
P.O. Box 51
N-2007 Kjeller, NORWAY

Dr. Peter Marshal
Procurement Executive
Ministry of Defense
Blacknest, Brimpton
Reading FG7-4RS, UNITED KINGDOM

Prof. Ari Ben-Menahem
Department of Applied Mathematics
Weizman Institute of Science
Rehovot, ISRAEL 951729

Dr. Robert North
Geophysics Division
Geological Survey of Canada
1 Observatory Crescent
Ottawa, Ontario, CANADA K1A 0Y3

Dr. Frode Ringdal
NTNF/NORSAR
P.O. Box 51
N-2007 Kjeller, NORWAY

Dr. Jorg Schlittenhardt
Federal Institute for Geosciences & Nat'l Res.
Postfach 510153
D-3000 Hannover 51, FEDERAL REPUBLIC OF GERMANY